Check for updates

Twinned *versus* linked organometallics - bimetallic "half-baguette" pentalenide complexes of Rh(I)†

Hugh J. Sanderson, [ID] [a] Gabriele Kociok-Köhn, [ID] [b] Claire L. McMullin [ID] [a] and Ulrich Hintermair [ID] *[a,c]

The application of **Mg[Ph₄Pn]** and **Li·K[Ph₄Pn]** in transmetalation reactions to a range of Rh(I) precursors led to the formation of "half-baguette" ***anti*-[Rhᴵ(L)ₙ]₂[μ:η⁵:η⁵Ph₄Pn]** (L = 1,5-cyclooctadiene, norbornadiene, ethylene; n = 1, 2) and ***syn*-[Rhᴵ(CO)₂]₂[μ:η⁵:η⁵Ph₄Pn]** complexes as well as the related iridium complex ***anti*-[Irᴵ(COD)]₂[μ:η⁵:η⁵Ph₄Pn]**. With CO exclusive *syn* metalation was obtained even when using mono-nuclear Rh(I) precursors, indicating an electronic preference for *syn* metalation. DFT analysis showed this to be the result of π overlap between the adjacent M(CO)₂ units which overcompensates for d_{z²} repulsion of the metals, an effect which can be overridden by steric clash of the auxiliary ligands to yield *anti*-configuration as seen in the larger olefin complexes. ***syn*-[Rhᴵ(CO)₂]₂[μ:η⁵:η⁵Ph₄Pn]** is a rare example of a twinned organometallic where the two metals are held flexibly in close proximity, but the two d⁸ Rh(I) centres did not show signs of M−M bonding interactions or exhibit Lewis basic behaviour as in some related mono-nuclear **Cp** complexes due to the acceptor properties of the ligands. The ligand substitution chemistry of ***syn*-[Rhᴵ(CO)₂]₂[μ:η⁵:η⁵Ph₄Pn]** was investigated with a series of electronically and sterically diverse donor ligands (P(OPh)₃, P(OMe)₃, PPh₃, PMe₃, dppe) yielding new mono- and bis-substituted complexes, with ***E-syn*-[Rhᴵ(CO)(P{OR}₃)]₂[μ:η⁵:η⁵Ph₄Pn]** (R = Me, Ph) characterised by XRD.

Introduction

The past decade has witnessed renewed interest in bimetallic complexes and the opportunities they offer in terms coopera-tive effects that derive from attractive or repulsive metal–metal interactions[1] within molecularly defined homometallic and heterobimetallic complexes of the s-, d- and f-block.[2–4] Bimetallics featuring Rh(I) are a particularly useful test for intermetallic effects due to its diamagnetic nature, useful [103]Rh coupling information, wide range of known mono-nuclear complexes and rich reactivity (stoichiometric as well as catalytic). The majority of known bimetallic Rh(I) complexes consist of a ligand with two distinct binding sites connected by a linker moiety, where the size and nature of the linker determines the proximity and the extent of electronic com-munication between the two Rh(I) centres.[5–19] With a view on

cooperative effects it is thus useful to distinguish between linked bimetallics (two monometallic complexes tethered together) and twinned bimetallics where the two metals are held closely enough for direct metal–metal interactions to exist.[20,21] This distinction is not purely a function of atomic distances but depends on orbital overlap and is thus a sliding scale akin to the Robin–Day classification,[22,23] where the extremes of a truly twinned bimetallic would be class III and a distantly linked bimetallic class I. A particularly interesting ligand platform to explore bimetallic effects is pentalenide (**Pn²⁻**, C₈H₆²⁻), the bicyclic analogue of cyclopentadienide (**Cp⁻**, C₅H₅⁻), itself one of the most widely used ligands in organometallic chemistry.[24] The bicyclic nature of **Pn²⁻** offers unique advantages over its monocyclic relative cyclooctatetrae-nide (**COT²⁻**, C₈H₈²⁻), including the formation of mono- and di-nuclear complexes paired with the ability to engage in a wide range of hapticities that allow for flexibility in the metal binding.[25] Monometallic **Pn²⁻** complexes often show folding around the central bridgehead carbon–carbon bond to engage in η⁸ bonding, a mode that thus far is exclusive to early d- and f-block metals with a d⁰ electron count.[26,27] Bimetallic **Pn²⁻** complexes can be classified as either *syn*- or *anti*-based on the relative orientation of the two metals, and can exhibit a range of coordination modes to **Pn²⁻** with η⁵/η⁵, η⁵/η³, η³/η³ and η⁵/η¹ known to exist.[27] The η¹/η¹ mode is also known for Si and Sn.[28–30] *Syn*-**Pn²⁻** complexes are most common for the homo-

[a]Department of Chemistry, University of Bath, Claverton Down, Bath BA2 7AY, UK. E-mail: u.hintermair@bath.ac.uk
[b]Material and Chemical Characterisation Facility, University of Bath, Claverton Down, Bath BA2 7AY, UK
[c]Institute for Sustainability, University of Bath, Claverton Down, Bath, BA2 7AY, UK

bimetallic double-sandwich (or perhaps more apposite, baguette) complexes of the type M_2Pn_2 which are known for Ti–Ni[31–35] as well as Rh and Pd.[36] Although intriguing compounds with regards to their structure, bonding and (photo) electrochemistry, in terms of chemical reactivity and potential use in bimetallic catalysis[1–4] the corresponding *syn*-bimetallic "half-baguette" complexes (analogous to the widely used mononuclear "half-sandwich" **Cp** complexes) would be very interesting to access and study. Several examples of such homobimetallic half-baguette complexes (M_2L_xPn) of Mn,[37,38] Fe,[39–43] Co,[43] Ni,[44] Ru,[45,46] Re[37,38] Rh and Ir[47] have been reported bearing a range of differently substituted pentalenide frameworks, including Pn^R (R = Ph, Me, NMe_2, H), 1,3-$(SiMe_3)_2Pn^{2-}$, 1,3,5-$(SiMe_3)_3Pn^{2-}$ and 1,2,3,4,5,6-Me_6Pn^{2-} (**Pn***). However, the factors that lead to *syn*/*anti* selectivity are not yet clear, nor have any of these complexes been used in ligand exchange reactions or catalysis. Intriguingly, the close proximity of two metals in *syn* bimetallic Pn^{2-} complexes can result in various and flexible degrees of metal–metal bonding. This can range from a double bond as in the homobimetallic baguette complex $[Ti(Pn^\dagger)]_2$ ($Pn^\dagger = 1,4-(^iPr_3Si)_2Pn$) which can undergo a wide range of reactivity including CO_2,[48,49] H_2 and CH activation,[50,51] to cases where the metal centres repel each other, such as *syn*-$[M(CO)_2]_2[Pn^\star]$ (M = Co, Rh, Ir) which were found to have M–M bond orders of −0.11, −0.06 and 0.16 for Co, Rh and Ir, respectively.[27,47] Further modulation of the reactivity within pentalenide complexes can be achieved by ligand exchange reactions. O'Hare and co-workers have derivatised their monometallic group 4 $Pn^{\star2-}$ dichloride complexes to introduce a variety of alkyl (Me, allyl, CH_2Ph), phenyl and amide (NMe_2, NPh_2) ligands to study their effects on stoichiometric CO_2 activation,[52–54] and similar modulation has allowed for the synthesis of group 4 mixed sandwich complexes.[55–57] However, auxiliary ligand exchange reactions of late d-block pentalenide complexes are unknown save for Manriquez and co-workers who reported that $[Cp^\star Ru^{II}(\mu:\eta^5:\eta^3Pn)Rh^I(COD)]$ will liberate COD to form $[Cp^\star Ru^{II}(\mu:\eta^5:\eta^3Pn)Rh^I(CO)_2]$ when exposed to a CO atmosphere.[58]

We have recently described the facile and modular syntheses of tetra-substituted dihydropentalenes[59] and introduced the first tetra-arylated pentalenide, $M_2[Ph_4Pn]$ (M = Li, Na, K)[60] and the first alkaline earth pentalenide, $Mg[Ph_4Pn]$.[61,62] The increased solubility and ease of separation of MgX_2 transmetalation by-products (through induced precipitation by addition of 1,4-dioxane[63,64]) are key advantages of $Mg[Ph_4Pn]$ over $M_2[Ph_4Pn]$ which make it a prime candidate to explore the coordination chemistry of Ph_4Pn^{2-} by way of salt metathesis. The majority of known pentalenide complexes contain pentalenide scaffolds containing electron-donating groups (such as alkyl and trialkylsilyl substituents), and the electron-withdrawing nature of the phenyl substituents should make Ph_4Pn^{2-} significantly less reducing and thus more suited to bind to electron-rich, late d-block metals. Indeed, recent DFT calculations have shown that the presence of the four phenyl groups reduces the HOMO–LUMO gap of Ph_4Pn^{2-} by 0.26 eV relative to Pn^{2-}

alongside a lowering in the absolute energy levels of both the HOMO and the LUMO (by 0.20 eV and 0.46 eV respectively).[65] The phenyl groups of Ph_4Pn^{2-} may allow for additional metal–arene interactions[66–68] that have not been seen with known (non-arylated) pentalenide complexes. In this work, we report the synthesis and characterisation of a series of bimetallic Rh(I) half-baguette pentalenide complexes and compare the outcome of transmetalation with $Mg[Ph_4Pn]$ to that of $Li\cdot K[Ph_4Pn]$. Furthermore, we explore the reactivity of a dirhodium tetracarbonyl complex (*syn*-$[Rh^I(CO)_2]_2[\mu:\eta^5:\eta^5Ph_4Pn]$) in ligand substitution reactions to evaluate the tolerance of the Ph_4Pn^{2-} scaffold to a range of donor and acceptor ligands.

Results and discussion

Synthesis and structure of *syn*- and *anti*-bimetallic Rh(I) and Ir(I) complexes

Synthesis of $[Rh^I(COD)]_2[Ph_4Pn]$ (1) and $[Ir^I(COD)]_2[Ph_4Pn]$ (2). Previous half-baguette Rh(I) and Ir(I) pentalenide complexes have required the use of stannylated pentalenides and low reaction temperatures to avoid unwanted redox chemistry between the electron-rich (reducing) $Pn^{\star2-}$ and the late d-block precursors.[47] In the case of the more π-accepting Ph_4Pn^{2-} this should be suppressed sufficiently to allow room temperature reactions without the need for "softer" stannylated derivatives which are highly toxic. To test this idea the reaction of $Mg[Ph_4Pn]$ and $[Rh^I(COD)(\mu-Cl)]_2$ was carried out at room temperature in THF which gave an immediate colour change from orange to dark red indicative of a transmetalation reaction. The ^1H NMR spectrum of the reaction mixture revealed full consumption of $Mg[Ph_4Pn]$ and showed the presence of a new singlet at 6.17 ppm (FWHM = 3.7 Hz) assigned to the two equivalent pentalenide wingtip protons (H_w) in a symmetrical transmetalation product. In THF-h_8 the COD signals were obscured by the solvent, however, redissolution into C_6D_6 showed three signals at 3.92 ppm, 2.08 ppm and 1.77 ppm, all shifted from those in the starting material $[Rh^I(COD)(\mu-Cl)]_2$. In C_6D_6 H_w was observed at 6.10 ppm (FWHM = 4.6 Hz) with a corresponding carbon (C_w) signal resolving as a doublet at 99.3 ppm with $^1J_{RhC}$ = 4.8 Hz, all indicative of the clean formation of $[Rh^I(COD)]_2[\mu:\eta^5:\eta^5Ph_4Pn]$ (1).

XRD analysis of single crystals of **1** grown from standing of a THF solution at −35 °C revealed the two rhodium(I) centres to be bound to Ph_4Pn^{2-} in an *anti*-geometry, with rhodium–C_5–centroid (Rh–C_t) distances of 1.9391(11) Å and 1.9502(11) Å (Fig. 1). The C_w–C_t–Rh angles of 86.4° and 87.4° suggested the Rh(I) centres to sit closer to the wingtip carbons than the bridgehead carbons (C_B), as also reflected in the corresponding Rh–C distances where the Rh–C_w distances were on average 0.15 Å shorter than the Rh–C_B distances. The heterobimetallic Pn^{2-} complex *anti*-$[Cp^\star Ru^{II}(\mu:\eta^5:\eta^3Pn)Rh^I(COD)]$ is the only other known pentalenide complex to contain a $Rh^I(COD)$ fragment, exhibiting Rh–C_t distances (1.944 Å) and Rh–C_t–C_w angles (86.6°) similar to that of **1** in the solid state but without any reported Rh–C_w coupling in solution.[58]
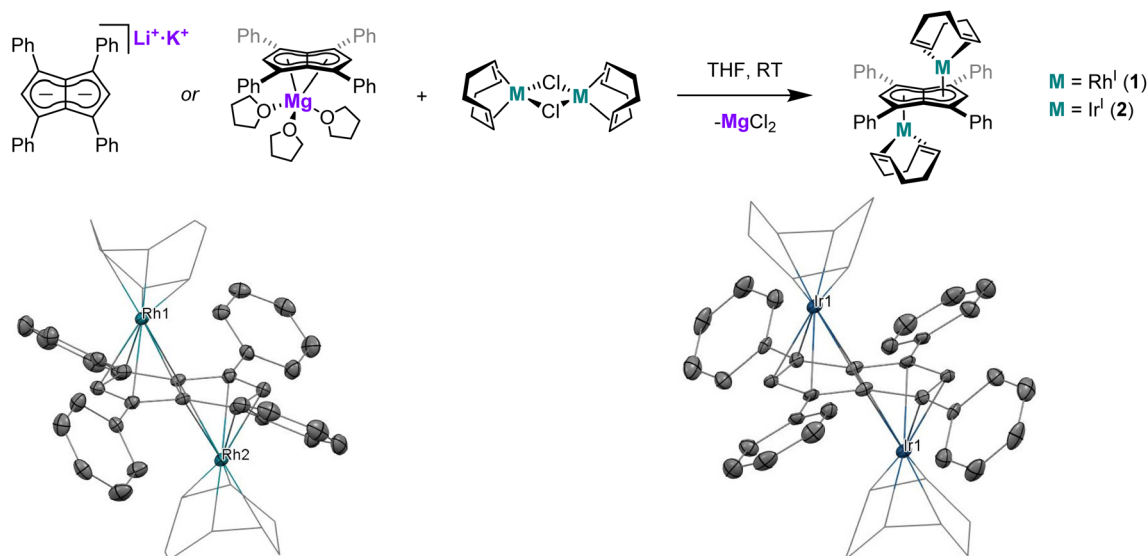
Fig. 1 Synthesis of *anti*-[Rh^I(COD)]$_2$[μ:η^5:η^{5}Ph$_4$Pn] (**1**) and *anti*-[Ir^I(COD)]$_2$[μ:η^5:η^{5}Ph$_4$Pn] (**2**) (top) and corresponding X-ray crystal structures with thermal ellipsoids at the 50% probability level (bottom; hydrogen atoms omitted for clarity).

Using the same procedure as described for **1**, the analogous reaction of [Ir^I(COD)(μ-Cl)]$_2$ with **Mg[Ph$_4$Pn]** resulted in the formation of the isostructural and isoelectronic complex *anti*-[Ir^I(COD)]$_2$[μ:η^5:η^{5}Ph$_4$Pn] (**2**). The two equivalent H$_w$ protons of **2** were found at the same chemical shift as in **1** (6.10 ppm in C$_6$D$_6$) but a 7 ppm upfield shift of C$_w$ was noticed in the Ir complex (92.3 ppm *vs.* 99.1 ppm for Rh). XRD analysis of single crystals of **2** confirmed the *anti*-geometry of the two iridium(ı) centres as in **1**. The M–C$_t$ distances in **2** (1.9241(19) Å, 1.9290(17) Å) were up to 0.026 Å shorter than in the rhodium complex **1** but otherwise the two compounds were iso-structural. The only previously reported iridium **Pn^{2-}** complex *syn*-[Ir^I(CO)$_2$]$_2$[μ:η^5:η^{5}Pn*]^{47} had an Ir–C$_t$ distance of 2.167 Å, significantly longer than in **2**. However, this difference is due to a combination of differences in the auxiliary ligands, **Pn^{2-}** frameworks, and geometry. **2** also exhibited some deviation towards C$_w$, as reflected in the shorter Ir–C$_w$ distances than the Ir–C$_B$ distances (by 0.17 Å) and the more acute C$_w$–C$_t$– Ir angles (86.3° and 86.9°), greater than what was noted for **1**.

Rh(ı) and Ir(ı) d^8 complexes typically prefer 16 e$^-$ configuration so a slight deviation from η^5 to η^3 may be expected, as η^5 coordination would yield a formal 18 e$^-$ count for each metal. The hapticity of the L$_3$X$_2$-type pentalenide ligand can be quantified with the displacement parameter Δ defined as the difference in the mean M–C$_B$ and M–C$_{NB}$ distances (C$_{NB}$ = nonbridgehead carbons).^{47,69,70} Relatively small ring slippage values of Δ = 0.13 and 0.15 can thus be calculated for **1** and **2**, respectively, which suggest a formal η^5 coordination of both Rh(ı) and Ir(ı) to **Ph$_4$Pn^{2-}**. The slightly larger value for **2** compared to **1** may be attributed to increased atomic size of Ir *versus* Rh.^{47} In contrast, the Rh centre in *anti*-[Cp*Ru^{II}(μ:η^5:η^{3}Pn)Rh^I(COD)] was reported as bound η^3 to **Pn^{2-}**, suggesting a formal 16 e$^-$ count. However, based on the XRD data reported for this complex, a value of Δ = 0.20 can be

calculated which is markedly less than what was reported for *syn*-[Rh^I(CO)$_2$]$_2$[Pn*] and that found for complex **5** (*vide infra*) which are both considered η^5 and thus 18 e$^-$ per Rh(ı). Complexes **1** and **2** also displayed close structural similarities to their mononuclear analogues [CpM^I(COD)] (M = Rh,^{71,72} Ir^{73}), with the COD ligand adopting the expected distorted boat conformation in all cases.

When the transmetalations of [Rh^I(COD)(μ-Cl)]$_2$ and [Ir^I(COD)(μ-Cl)]$_2$ were performed using **Li·K[Ph$_4$Pn]**^{60} instead of **Mg[Ph$_4$Pn]**, the same colour changes (dark red for Rh, dark yellow for Ir) were observed and analysis by ^{1}H and ^{13}C{^{1}H} NMR spectroscopy confirmed the formation of **1** and **2**, respectively (Fig. S4, S5, S9 and S10†). This observation showed that the nature of the counter cation(s) of **Ph$_4$Pn^{2-}** does not influence the outcome of transmetalation reactions in donor solvents such as THF where these salts exist as solvent-separated ion pairs, despite the formal presence of a LiCp-like unit^{60} which was found to be too reducing in the case of reacting **Li$_2$[Pn*]** with Rh(ı) and Ir(ı) precursors.^{47} This difference in reactivity likely reflects the electronic nature of the pentalenide used, in line with recent calculations showing **Ph$_4$Pn^{2-}** to have significantly lower frontier orbital energies than **Pn^{2-}** and its alkylated derivatives,^{65} making it a less reducing π base (donor) and a better π acid (acceptor).

Synthesis of [Rh^I(NBD)]$_2$[Ph$_4$Pn] (3) and [Rh^I(C$_2$H$_4$)$_2$]$_2$[Ph$_4$Pn] (4). With the COD precursors yielding *anti*-isomers, it was interesting to extend the transmetalation to other olefinic precursors that possess a smaller steric profile than COD to see if the selectivity of the transmetalation was dictated by sterics. Therefore, the reaction of [Rh^I(NBD)(μ-Cl)]$_2$ with **Mg[Ph$_4$Pn]** was carried out which led to the formation of *anti*-[Rh^I(NBD)]$_2$[μ:η^5:η^{5}Ph$_4$Pn] (**3**) (Fig. 2). Compared to **1** and **2**, a slower formation of complex **3** was noticed with the colour change from orange to bright yellow occurring over the course
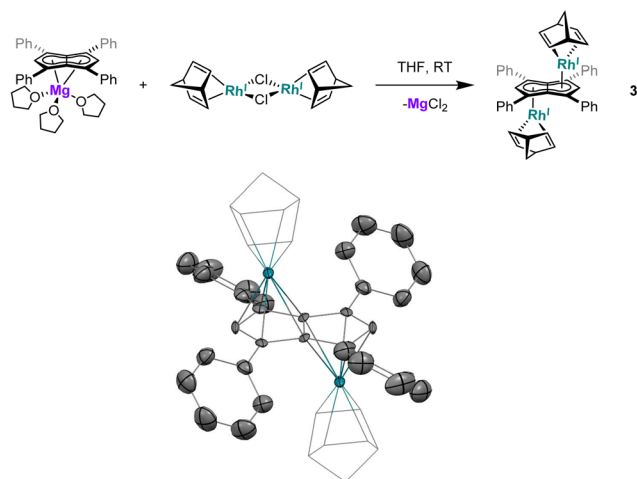
Fig. 2 Synthesis of *anti*-[Rh^I(NBD)]$_2$[μ:η^5:η^{5}Ph$_4$Pn] (**3**) (top) and its X-ray crystal structure with thermal ellipsoids at the 50% probability level (bottom; hydrogen atoms omitted for clarity).

Fig. 3 Synthesis of *anti*-[Rh^I(C$_2$H$_4$)$_2$]$_2$[μ:η^5:η^{5}Ph$_4$Pn] (**4**) (top) and its X-ray crystal structure with thermal ellipsoids at the 50% probability level (bottom; hydrogen atoms omitted for clarity).

of several of minutes at room temperature. The ^{1}H NMR spectrum of the solution showed a new **Ph$_4$Pn^{2-}** environment with the emergence of a new **H$_w$** signal resolved as a doublet at 6.22 ppm ($^2J_{RhH}$ = 0.8 Hz). The associated carbon shift, **C$_w$**, was also resolved as a doublet in the ^{13}C{^{1}H} NMR spectrum at 97.4 ppm ($^1J_{RhC}$ = 5.8 Hz). XRD analysis of single crystals of **3** showed the two Rh(I) centres to be located *anti* to each other as in **1** bearing COD instead of NBD (Fig. 2). The Rh–C$_t$ distance of 1.938(3) Å in **3** was near identical to that of **1**, and the Rh–C$_t$–C$_w$ angle of 86.1° was marginally smaller than in **1**. The ring slippage value of 0.15 was the same as in **1** and the rhodium thus best described as bonded η^5 to **Ph$_4$Pn^{2-}**.

Utilising the ethylene complex [Rh^I(C$_2$H$_4$)$_2$(μ-Cl)]$_2$ featuring a minimally substituted, monodentate olefin ligand in a transmetalation with **Mg[Ph$_4$Pn]** in THF resulted in an immediate colour change from orange to dark yellow. The ^{1}H NMR spectrum of the mixture revealed the appearance of a new **H$_w$** signal at 6.21 ppm, indicating successful transmetalation. After 10 minutes a black solid started to form, presumed to be elemental rhodium from decomposition, indicating the product to be unstable at room temperature. Lower temperatures and lower polarity solvents did not fully prevent this decomposition but slowed it sufficiently for analysis. In C$_6$D$_6$ **H$_w$** of the product appeared as a doublet at 5.98 ppm ($^2J_{RhH}$ = 0.7 Hz), 0.1–0.2 ppm upfield relative to the COD and NBD analogues. In the ^{13}C{^{1}H} NMR spectrum **C$_w$** was resolved as a doublet at 98.6 ppm ($^1J_{RhC}$ = 5.2 Hz), suggesting the electronics of the COD, NBD and ethylene complexes to be very similar. Crystals of **4** could be grown from the reaction mixture at −35 °C after MgCl$_2$ had been removed *via* addition of dioxane and filtration. Complex **4** was found to be isostructural to **1** and **3** by XRD (Fig. 3), with an *anti*-configuration and Rh–C$_t$ distances of 1.9408(9) Å and 1.9383(9) Å, and Rh–C$_t$C$_w$ angles of 86.6° and 87.8°.

Synthesis of [Rh^I(CO)$_2$]$_2$[Ph$_4$Pn] (5). The formation of the linked *anti*-bimetallics **1–4** suggested that to access a twinned
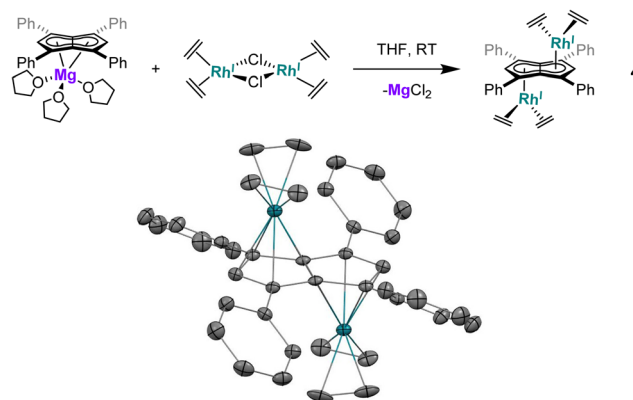
syn-Rh(I) bimetallic pentalenide complex a different auxiliary ligand would be needed. [Rh^I(CO)$_2$(μ-Cl)]$_2$ has previously been used to give the *syn*-dirhodium complex **[Rh^I(CO)$_2$]$_2$[Pn*]**[47] and as such the **Ph$_4$Pn^{2-}** analogue was targeted. Addition of a THF solution of [Rh^I(CO)$_2$(μ-Cl)]$_2$ to either **Mg[Ph$_4$Pn]** or **Li·K[Ph$_4$Pn]** gave an immediate colour change to dark yellow (Fig. 4) and the corresponding ^{1}H NMR spectrum revealed a new **Ph$_4$Pn^{2-}** environment with a slight shift in **H$_w$** to a doublet at 6.91 ppm ($^2J_{RhH}$ = 1.4 Hz) from the singlet at 6.80 ppm in **Mg[Ph$_4$Pn]**. In the ^{13}C{^{1}H} NMR spectrum the associated **C$_w$** was found to be a doublet at 90.1 ppm ($^1J_{RhC}$ = 7.0 Hz) and was shifted slightly downfield relative to complexes **1–4**, likely a result of the increased acceptor ability of CO compared with COD, NBD and ethylene. The monometallic analogue of **5**, **[Rh^I(CO)$_2$(Ph$_2$Cp)]** has been reported to have a ^{1}H NMR signal at 5.99 ppm with a coupling constant of $^2J_{RhH}$ = 0.5 Hz (C$_6$D$_6$) for the **Cp** proton between the two phenyl rings,[74] suggesting **Ph$_4$Pn^{2-}** to be a better acceptor ligand that binds more strongly to Rh(I) than **Ph$_2$Cp$^-$**. The ^{13}C{^{1}H} NMR
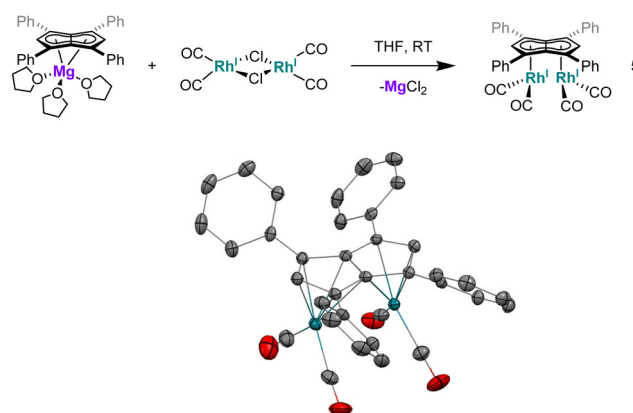

Fig. 4 Synthesis of *syn*-[Rh^I(CO)$_2$]$_2$[μ:η^5:η^{5}Ph$_4$Pn] (**5**, top) and its X-ray crystal structure with thermal ellipsoids at the 50% probability level (bottom; hydrogen atoms omitted for clarity).

spectrum of **5** showed a doublet at 194.5 ppm ($^1J_{RhC}$ = 83.8 Hz) for the carbonyl groups, consistent with **[(Rh^I(CO)$_2$(Ph$_2$Cp)]** and **[Rh^I(CO)$_2$]$_2$[Pn*]**, though in the latter a much smaller coupling constant of $^1J_{RhC}$ = 49.1 Hz was reported. However, the IR data suggests a stronger Rh–CO bond in **[Rh^I(CO)$_2$]$_2$[Pn*]** than in **5** consistent with increased donor ability of **Pn*$^{2-}$** compared to **Ph$_4$Pn^{2-}** (Table 1).

The X-ray crystal structure of **5**, depicted in Fig. 4, confirmed a *syn*-dirhodium arrangement. A comparison of the key structural features with ***syn*-[Rh^I(CO)$_2$]$_2$[Pn*]** as well as complexes **1–4** can be found in Table 2. As in the **Pn*$^{2-}$** analogue, the two Rh^I(CO)$_2$ fragments were located next to each other on the **Ph$_4$Pn^{2-}** with an intermetallic distance of 2.9130(4) Å, too long to ascribe any direct Rh–Rh interaction[36,47] as also reflected in a formal shortness ratio (FSR) of 1.16 using a R_1 value of 1.247.[76,77] O'Hare related this increased distance to the C$_5$ rings of **Pn*$^{2-}$** being partially bent away at a hinge angle of 11.4° (defined as the angle between the plane of the **C$_w$** and non-wingtip carbons (**C$_{NW}$**) and the plane of C$_{NW}$ and C$_B$),[47] with DFT analysis showing the HOMO of **[Rh^I(CO)$_2$]$_2$[Pn*]** to contain a Rh–Pn* antibonding component that is offset by the Rh–CO π-backdonation.[27,47] **5** exhibited a smaller hinge angle of 10.2° due to the increased π-accepting ability of the phenyl substituents in **Ph$_4$Pn^{2-}**. However, despite the changes in electronics of the pentalenide ligand an identical ring slippage value of Δ = 0.27 was found. This is noticeably larger than for the *anti*-complexes **1–4** signifying a greater deviation towards η^3 in the *syn*-systems, further evidenced by the more acute Rh–C$_t$–C$_w$ angles of 82.4° and 82.6°, suggesting some electronic repulsion between the Rh^I(CO)$_2$ fragments. While complex **4** had a L–Rh–L *versus* pentalenide dihedral angle of 86.1° (close to the ideal 90° geometry, Fig. S61†), in **5** the two L–Rh–L units were angled at 77.8° relative to the pentalenide. This outward bending together with the greater Δ value towards η^3

and 10.2° pentalenide hinging in **5** all contribute to an enlarged Rh–Rh distance signifying intermetallic repulsion. Previous DFT analysis of **[Rh^I(CO)$_2$]$_2$[Pn*]** had revealed an out of phase interaction of the metal d$_{z^2}$ orbitals in the HOMO−1 leading to a formal negative bond order of −0.06.[27,47]

The average Rh–CO bond length found in **5** was 1.876(1) Å, 0.01 Å longer than in ***syn*-[Rh^I(CO)$_2$]$_2$[Pn*]** suggesting less Rh–CO backbonding in **5**. This was further supported by IR spectroscopy where **5** exhibited four carbonyl bands at 1992, 2025, 2046 and 2064 cm^{-1}, similar to what was reported for **[Rh^I(CO)$_2$(Ph$_2$Cp)]** (1962 and 2040 cm^{-1}),[74] and shifted to higher wavenumbers compared to ***syn*-[Rh^I(CO)$_2$]$_2$[Pn*]**[47] indicative of a stronger CO bond and weaker Rh–CO backbonding as a reflection of the increased π-accepting ability of **Ph$_4$Pn^{2-}** over **Pn*$^{2-}$**.

Interested in whether the formation of the *syn*-isomer was partially influenced by the use of a dimeric rhodium precursor, the reaction was repeated with the monomeric [Rh^I(acac)(CO)$_2$], with the formation of **5** confirmed by NMR and IR spectroscopy. Moreover, the influence of the cation was found to be negligible as the reaction of either [Rh^I(acac)(CO)$_2$] or [Rh^I(CO)$_2$(μ-Cl)]$_2$ with **Li·K[Ph$_4$Pn]** also resulted in clean formation of **5** (Scheme 1).

Electronic structure and reactivity

To gain deeper insight into the origin of *syn versus anti* formation on **4** and **5**, comparative Density Functional Theory (DFT) calculations were carried out on ***syn*-4**, ***anti*-4**, ***syn*-5** and ***anti*-5** (see ESI† for details). The optimised geometries of ***anti*-4** and ***syn*-5** showed good agreement with the crystallographic data, and ***anti*-4** was found to be 1.2 kcal mol^{-1} lower in energy than ***syn*-4** whereas ***syn*-5** was 4.6 kcal mol^{-1} more stable than ***anti*-5**. These results are fully in line with our experimental findings and show *syn/anti* selectivity in the transmetalation of

---

**Table 1** Key NMR and IR data of complex **5** and related literature compounds

	δ H$_w$/ppm	δ C$_w$/ppm	δ CO/ppm	ν_{CO}/cm^{-1}
[Rh(CO)$_2$]$_2$[Ph$_4$Pn] (5)	6.91 ($^2J_{RhH}$ = 0.45 Hz)	90.1 ($^1J_{RhC}$ = 6.96 Hz)	194.5 ($^1J_{RhC}$ = 83.8 Hz)	2064, 2046, 2025,
[Rh(CO)$_2$(Ph$_2$Cp)][74]	5.99 ($^2J_{RhH}$ = 0.45 Hz)	83.7 ($^1J_{RhC}$ = 3.17 Hz) and 85.4 ($^1J_{RhC}$ = 3.64 Hz)	191.3 ($^1J_{RhC}$ = 84.0 Hz)	2040, 1962
[Rh(CO)$_2$]$_2$[Pn*][47]	n/a	71.0	196.3 ($^1J_{RhC}$ = 49.1 Hz)	2034, 1999, 1965, 1946[b]
[Rh(CO)$_2$][Cp*][75]	n/a	n/a	195.1 ($^1J_{RhC}$ = 75.6 Hz)[a]	2016, 1948

[a] Calculated from reported NMR data. [b] IR data recorded using a KBr pellet.

Table 2 Key NMR and structural parameters of complexes **1–5** and related literature compounds

	δ H$_w$/ppm	δ C$_w$/ppm	M-M/Å	M-C$_t$/Å	M-C$_t$-C$_w$/ °	Ring slippage Δ
***anti*-[Rh^I(COD)]$_2$[Ph$_4$Pn] (1)**	6.17	99.3 ($^1J_{RhC}$ = 5 Hz)	4.5305(5)	1.9391(11), 1.9502(11)	86.4, 87.4	0.11, 0.15
***anti*-[Ir^I(COD)]$_2$[Ph$_4$Pn] (2)**	6.28	93.6	4.5411(5)	1.9241(19), 1.9290(17)	86.3, 86.9	0.15
***anti*-[Rh^I(NBD)]$_2$[Ph$_4$Pn] (3)**	6.22 ($^2J_{RhH}$ = 0.8 Hz)	97.4 ($^1J_{RhC}$ = 6 Hz)	4.5462(9)	1.938(3)	86.1	0.15
***anti*-[Rh^I(C$_2$H$_4$)$_2$]$_2$[Ph$_4$Pn] (4)**	5.98 ($^2J_{RhH}$ = 0.7 Hz)	98.6 ($^1J_{RhC}$ = 5 Hz)	4.4862(3)	1.9383(9), 1.9408(9)	86.6, 87.8	0.14, 0.10
***anti*-[Cp*Ru^{II}(μ:η^5:η^{3}Pn)Rh^I(COD)][58]**	5.84	n/a	4.4166(4)	1.944	86.6	0.20
***syn*-[Rh^I(CO)$_2$]$_2$[Ph$_4$Pn] (5)**	6.50 ($^2J_{RhH}$ = 1.7 Hz)	89.8 ($^1J_{RhC}$ = 7 Hz)	2.913(6)	1.9917(9), 1.9940(9)	82.4, 82.6	0.27
***syn*-[Rh^I(CO)$_2$]$_2$[Pn*][47]**	n/a	n/a	2.9130(4)	1.976	83.0, 83.1	0.27
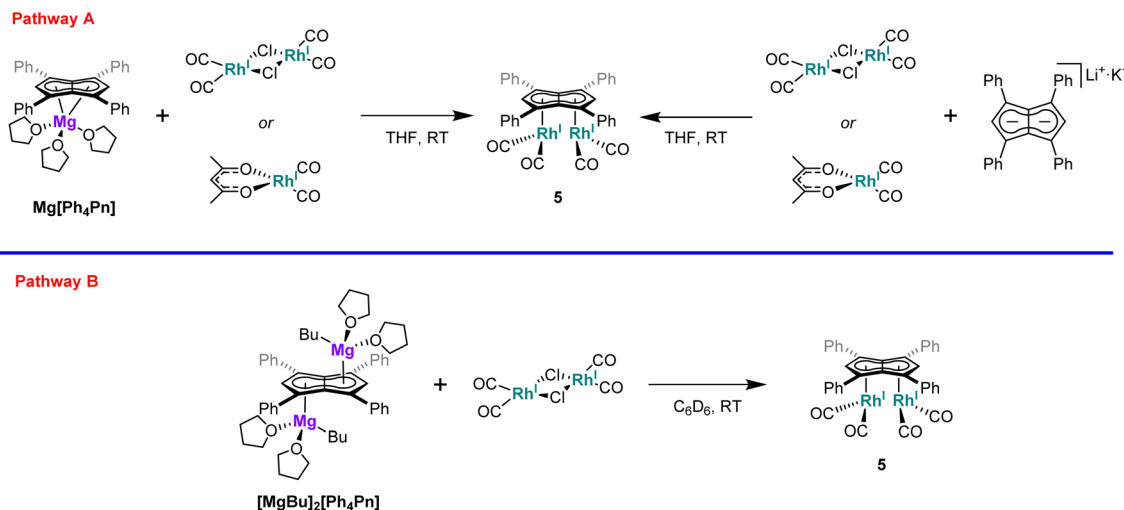
Scheme 1 Synthetic pathways to [Rh^I(CO)$_2$]$_2$[Ph$_4$Pn].

solvent-separated group 1 and group 2 pentalenide salts with Rh(I) and Ir(I) precursors to be thermodynamically controlled. NBO calculations on **syn-4** and **syn-5** returned Wiberg Bond Index (WBI) values of 0.06 and 0.05 between the two Rh(I) centres, respectively, indicating no significant M–M interactions. As reported for the **Pn*$^{2-}$** system,[47] the HOMO−1 of **syn-5** contained an out-of-phase (repulsive) interaction between the Rh d$_{z^2}$ orbitals, whilst an in-phase (attractive) interaction between the two co-planar Rh(CO)$_2$ moieties was found in the HOMO of **syn-5** (Fig. 5). Interestingly, the HOMO of **syn-4** contained a similar positive interaction between the two adjacent Rh(C$_2$H$_4$)$_2$ moieties (Fig. 6), suggesting that there is a general energetic preference for *syn*-metallation in pentalenide complexes of Rh(I) and Ir(I) with π acceptor ligands despite a repulsive M–M interaction. As the switch in isomer preference from *syn* to *anti* when going from CO to C$_2$H$_4$ shows, steric clashing between the ancillary ligands easily overrides the net electronic preference for *syn* to yield *anti*-geometry in a bimetallic more akin to two linked (or fused) **Cp** complexes.

To investigate whether the orientation of the metals resulted in any significant changes in their electronic structure the UV-vis spectra of **1**, **5** and the monomeric derivative of **5**, **[Rh^I(CO)$_2$(Ph$_2$Cp)]** were recorded in THF (Fig. S25†). All three displayed peaks attributable to π–π* transitions of the π-ligands (320 nm for **1** and **5**, 350 nm for **[Rh(CO)$_2$(Ph$_2$Cp)]**), with a slight red shift for the monometallic complex also observed in the group 1 salts of **Ph$_4$Pn^{2-}** and **Ph$_2$Cp$^−$**,[60] suggesting the orientation of the metals to have negligible influence on the main electronic transitions.

Given the repulsive d$_{z^2}$ interactions found in the HOMO−1 of the twinned *syn* bimetallics, we tested the influence of the metal orientation on the Lewis basicity of ***anti*-3** and **syn-5**. Related mononuclear four-coordinate d^8 complexes are known to display nucleophilic behaviour by virtue of their filled, non-bonding d$_{z^2}$ orbital which may act as a σ-donor to a range of Lewis acids.[78] This effect has even been seen (and exploited for intermetallic reactivity in metal-based Lewis pairs[79–82]) in formally five-coordinate 18 electron η^5-CpRh(I) complexes that

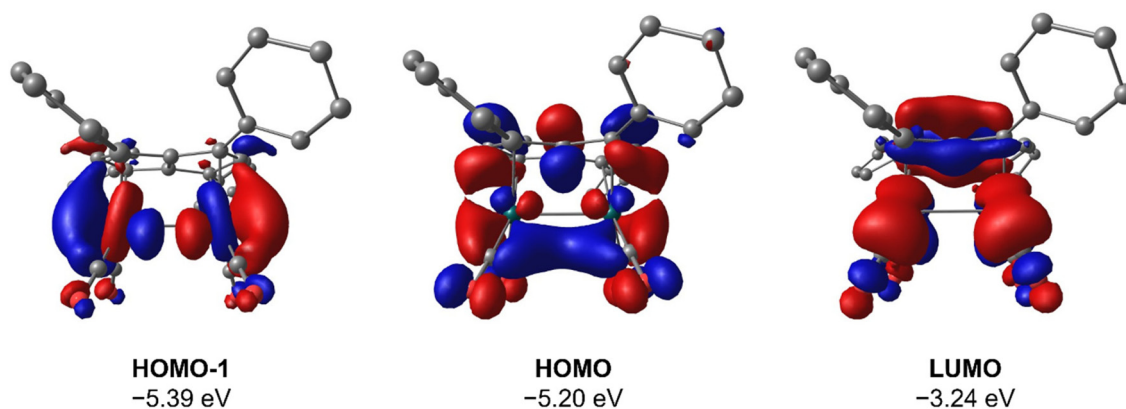**HOMO-1** −5.39 eV   **HOMO** −5.20 eV   **LUMO** −3.24 eV

Fig. 5 HOMO−1, HOMO and LUMO of *syn*-[Rh(CO)$_2$]$_2$[Ph$_4$Pn] (**syn-5**) at the BP86/BS2//BP86/BS1 level of theory. Hydrogen atoms omitted for clarity.

HOMO−1
−5.01 eV

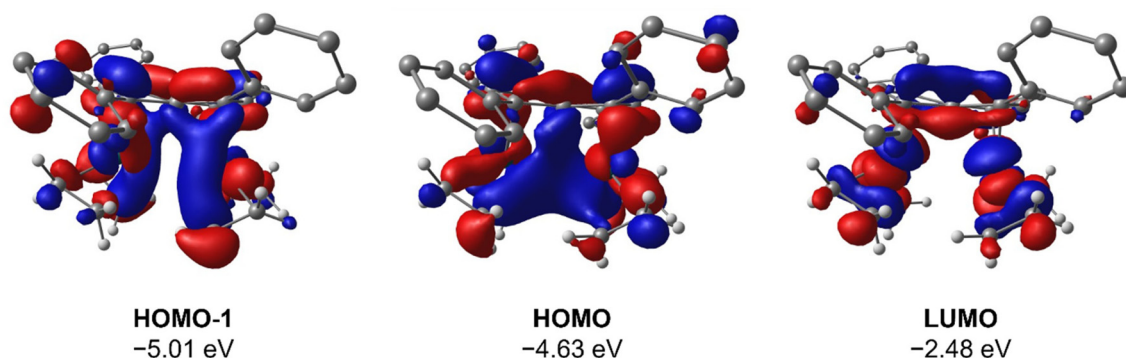**HOMO**
−4.63 eV

LUMO
−2.48 eV

Fig. 6 HOMO−1, HOMO and LUMO of *syn*-[Rh(C$_2$H$_4$)$_2$]$_2$[Ph$_4$Pn] (*syn*-4) at the BP86/BS2//BP86/BS1 level of theory. Hydrogen atoms of the pentalenide omitted for clarity.

have an empty, non-bonding d$_{z^2}$ orbital,[79] where their nucleophilic behaviour may either arise from an electron-rich Rh–L bond or a temporary η^5–η^3 slip of the **Cp** ligand. However, addition of AlCl$_3$ to ***anti*-3** and ***syn*-5** in THF showed no changes in their ^{1}H NMR spectra even after one week at room temperature. Control reactions with **1** and **[Rh^I(CO)$_2$(Ph$_2$Cp)]** also showed no reactivity with AlCl$_3$, highlighting the low nucleophilicity of these complexes which may be ascribed to the phenyl groups lowering the HOMO and LUMO of the **Pn^{2-}** and increase the π-acceptor character of the ligand.[65] This is in contrast to the electron-rich Rh(I) complexes furnished with strongly σ-donating phosphines (*e.g.* PMe$_3$) and electron rich π-ligands (*e.g.* **Cp***) which serve to raise the energy of the HOMO and thus increase their nucleophilicity.[83–85]

Ligand substitution chemistry of [Rh^I(CO)$_2$]$_2$[Ph$_4$Pn] (5)

N-donor ligands. Interested in modulating the reactivity and electronic structure of the twinned bimetallic **5** by ligand exchange (either symmetrically or asymmetrically) we explored the introduction of N-based donor ligands. **CpRh^I(bipy)** complexes are well-known compounds with interesting redox properties such as facile switching between Rh(ɪ) and Rh(ɪɪɪ) which has been utilised in a wide range of applications.[86–92] However, the addition of two equivalents of bipy to a THF solution of **5** led to no change in the NMR spectra even after adding an excess and heating the mixture to 50 °C for one week (Scheme 2, and Fig. S26†). Performing the analogous reaction with pyridine yielded the same result, and even photolytic conditions[93] (exposure to 150 W white light for one hour)

did not allow displacement of the carbonyls of **5** with N-donor ligands.

This surprising inertness of **5** either reflects either a kinetic barrier due to steric shielding by the phenyl substituents of the pentalenide or a thermodynamic preference of the complex for strong acceptor ligands like CO. To probe this question further we tried to introduce a range of P-donor ligands with varying degrees of donor/acceptor abilities.

P-donor ligands

Phosphines. The addition of one equivalent of PPh$_3$ to **5** in THF led to no discernible colour change over several days at room temperature, however, the ^{1}H NMR spectrum showed a desymmetrisation of the pentalenide ligand consistent with monosubstitution to form **[Rh^I(CO)$_2$;Rh^I(CO)(PPh$_3$)][μ:η^5:η^{5}Ph$_4$Pn]** (6) (Scheme 3). Two singlets at 6.23 ppm and 6.71 ppm in the ^{1}H NMR spectrum could be assigned to two new wingtips **H$_{wa}$** and **H$_{wb}$** respectively (as confirmed by ^{1}H-^{31}P HMBC), indicating an electronically asymmetric **Ph$_4$Pn^{2-}** environment with one C$_5$-ring bound to a more electron-rich Rh^I(CO)(PPh$_3$) fragment and one C$_5$-ring bound to a more electron-deficient Rh^I(CO)$_2$ fragment. This was reflected with the chemical shift of **H$_{wb}$** being closer to that of **H$_w$** in **5**, with the slight upfield shift of 0.2 ppm reflective of the delocalised electronic nature of the **Ph$_4$Pn^{2-}** anion. The ^{31}P{^{1}H} NMR spectrum of **6** revealed a doublet centered at 48.1 ppm ($^1J_{RhP}$ = 202 Hz), similar to that reported for **[CpRh^I(CO)(PPh$_3$)]** (52.7 ppm, $^1J_{RhP}$ = 199.5 Hz).[94] The UV-vis spectrum of **6** displayed similar π–π* transitions of the **Ph$_4$Pn^{2-}** in the UV region around 300 nm to that of **5**, however, with an additional
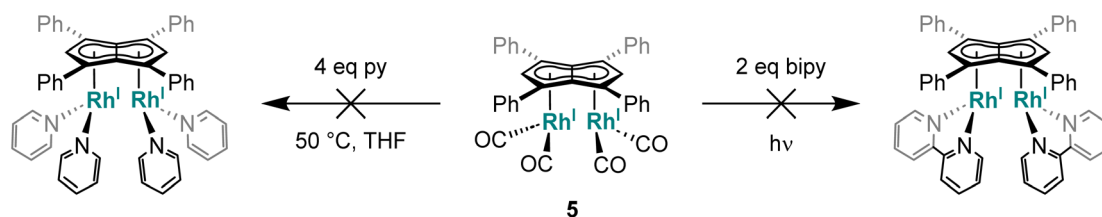
Scheme 2 Attempted introduction of pyridyl ligands to *syn*-[Rh^I(CO)$_2$]$_2$[Ph$_4$Pn].
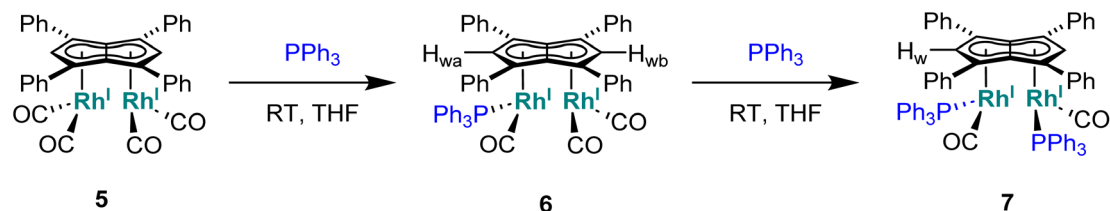
Scheme 3 Synthesis of mono and bis-triphenylphosphine derivatives of *syn*-[Rh^I(CO)$_2$]$_2$[Ph$_4$Pn] (**5**).

broad band centred at 838 nm (ε = 7383 M^{-1} cm^{-1}) which was absent for the symmetrical complexes **5** and **11** (Fig. S56 and 57†) and indicated intermetallic charge transfer between the electronically inequivalent Rh(I) centres in **6**.[22,23]

When two equivalents of PPh$_3$ were added to **5**, initially only the monosubstituted complex **6** was observed in the ^{1}H and ^{31}P{^{1}H} NMR spectra of the solution (Fig. S31†), but over the course of 12 hours the emergence of a new doublet at 51.4 ppm ($^1J_{RhP}$ = 198 Hz) along with the diminishing of the signals assigned to **6** was observed in the ^{31}P{^{1}H} NMR spectrum. The new signal is ascribed to the symmetrically disubstituted product **7**, but full characterisation was impeded by the transformation not going to completion and all attempts at isolating **7** from the dynamic mixture being unsuccessful. The electronic similarity of **7** to **6** and to [CpRh^I(CO)(PPh$_3$)][94] reflected in their NMR data strongly suggested each Rh^I(CO)$_2$ centre underwent mono-substitution instead of one Rh^I(CO)$_2$ centre undergoing double substitution to yield a species akin to [CpRh^I(PPh$_3$)$_2$] (^{31}P = 57.3 ppm, $^1J_{RhP}$ = 222

Hz).[95] Using more than two equivalents of PPh$_3$ per **5** led to complex mixtures that contained **6** and **7** but also a multitude of other products (Fig. S31†), showing the introduction of phosphines to be more easily achievable than pyridines albeit with some barrier likely arising from steric hindrance (PPh$_3$ being much larger than CO).

When the smaller and more σ-donating trimethylphosphine was employed in place of PPh$_3$ a colour change from the dark yellow of **5** to red was noticed over the course of five minutes at room temperature. The ^{31}P{^{1}H} NMR spectrum of this solution showed a signal centred at −24.0 ppm with second order coupling, indicative of a rhodium-phosphorous dimer (Fig. S34†).[96] Two broad peaks at −16.2 ppm and −34.4 ppm were also observed suggesting some fluxionality within the product(s) formed. Although all attempts at isolating a clean sample lead to decomposition, standing of a 1 : 1 THF/pentane solution of the crude reaction mixture at −35 °C overnight led to the formation of crystals of the ion pair [Rh^{II}(CO)(PMe$_3$)$_4$][Ph$_4$Pn] (**8**, Fig. 7) where four PMe$_3$ ligands had
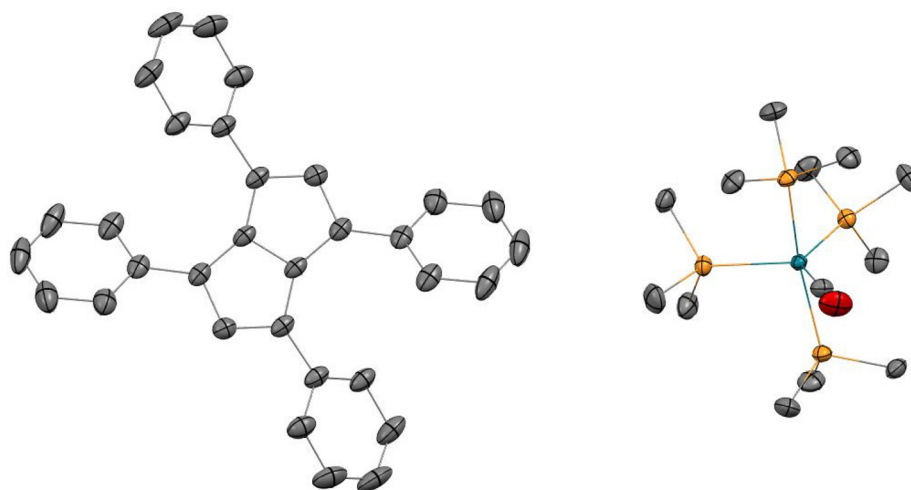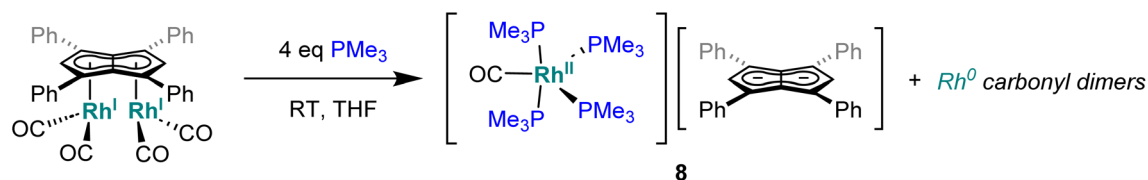

Fig. 7 Synthesis of [Rh^{II}(PMe$_3$)$_4$(CO)][Ph$_4$Pn] (**8**) (top) and its X-ray crystal structure with thermal ellipsoids at the 50% probability level (bottom; hydrogen atoms omitted for clarity).

detached the Rh-carbonyl centre from the pentalenide. To the best of our knowledge this is the first crystallographically characterised uncomplexed pentalenide and exhibits a perfectly co-planar core with the phenyl rings twisted by 21.2°–26.8° to minimise steric repulsion between adjacent rings and allow some conjugation of the charge into the phenyl substituents. This rotation is less than what was found for **Li₂[Ph₄Pn]**[60] (29.3°–35.8°) but within the range seen for **Mg[Ph₄Pn]** (17.1°–35.2°).[61]

The cationic fragment of **8** consisted of a Rh(II) centre in a distorted trigonal bipyramidal geometry with PMe₃ groups occupying both axial and two equatorial positions with one carbonyl group occupying the third equatorial site. Exchange between the equatorial and axial positions is likely responsible for the observation of two inequivalent, broad signals in the $^{31}P\{^1H\}$ NMR spectra, although variable temperature NMR data were inconclusive (Fig. S35†) due to the paramagnetic nature of Rh(II) which was independently confirmed by the Evans method (Fig. S36†). In the solid state, the Rh–P$_{eq}$ bonds were 0.056 Å longer than Rh–P$_{ax}$ bonds (2.3227(4)–2.3859(7) Å), with the axial PMe₃ groups bent away from the equatorial PMe₃ to give a P$_{ax}$–Rh–P$_{ax}$ angle of 165.6° to relive steric clash between the methyl groups. The related cation $[Rh^I(CO)(PMe_3)_4]^+$ has previously been reported,[97] however, with no spectroscopic or crystallographic data provided. Mononuclear Rh(II) complexes are uncommon and often adopt square planar or octahedral geometries in the presence of bulky chelating ligands with 15 e⁻ or 19 e⁻ counts, respectively,[98–104]

whereas the cation of **8** is a rare example of a five-coordinate 17 electron complex with monodentate ligands only. The formation of a dicationic Rh(II) complex from the two adjacent Rh(I) centres in **5** is likely the result of a disproportionation reaction induced by the introduction of the strongly σ-donating PMe₃ ligand, producing dimeric Rh(0) carbonyl species responsible for the signal at −24.0 ppm in the $^{31}P\{^1H\}$ NMR spectrum of the product mixture.

To see if a bidentate ligand would span across the two rhodium centres (μ²) or chelate around a single metal (κ²) in **5** the introduction of bis(diphenylphosphino)ethane (dppe) was tested. Whereas the ¹H NMR spectrum showed no significant change in the position of **H$_w$** after adding dppe to **5** in THF, the $^{31}P\{^1H\}$ NMR spectrum showed a new doublet at 57.6 ppm ($^1J_{RhP}$ = 128.3 Hz) with **C$_w$** still exhibiting rhodium-carbon coupling. Crystals suitable for XRD, grown from standing of the reaction mixture at −35 °C, revealed the formation of the non-contact ion pair $[Rh^I(dppe)_2][Rh^I(CO)_2(\eta^5Ph_4Pn)]$ (**9**, Fig. 8) where one Rh(I) centre was bound to **Ph₄Pn²⁻** in an η⁵ coordination fashion with a Rh-C$_t$ distance of 1.959(2) Å, 0.35 Å shorter than the equivalent distance in the di-Rh(I) complex **5**. This significant shortening likely is a consequence of the monometallic coordination of Rh^I(CO)₂ to **Ph₄Pn²⁻** leading to increased interaction of the cationic d⁸ centre with the dianionic 10π system. There was also less pronounced deviation to η³ in **9** compared to **5**, as evidenced by the slight increase in the Rh–C$_t$–C$_w$ angle (84.1° vs. an average 82.5° in **5**) and a decrease in the ring slippage value Δ = 0.23 (cf. 0.27 in
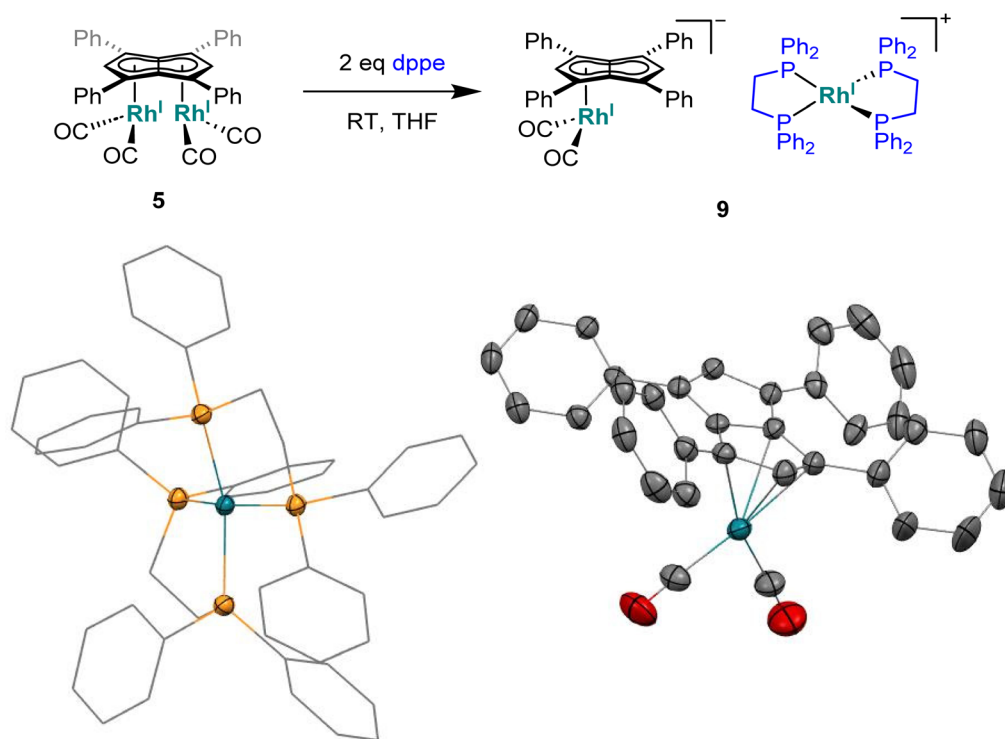

Fig. 8 Synthesis of $[Rh^I(dppe)_2][Rh^I(CO)_2(\eta^5Ph_4Pn)]$ (**9**) (top) and its X-ray crystal structure with thermal ellipsoids at the 50% probability level (bottom; hydrogen atoms omitted for clarity).

5). Moreover, a smaller hinge angle of 8.4° was found for **9**, presumably due to a relaxation of **Ph₄Pn²** and the loss of steric strain from *syn*-dimetallation, whilst the uncomplexed C₅-ring exhibited a hinge angle of 2°. The Rh–CO distances in **9** were also 0.016 Å shorter than in **5** suggesting a greater degree of back-bonding in the former, which was further supported by the IR spectrum of **9** exhibiting two CO bands at 1980 cm⁻¹ and 1918 cm⁻¹ (Fig. S41†). The [Rhᴵ(CO)₂(η⁵Ph₄Pn)] anion could also be crystallised with a [Mg₂Cl₃(THF)₆] cation when MgCl₂ was not removed by addition of dioxane prior to dppe addition (Fig. S42†). The cationic [Rhᴵ(dppe)₂]⁺ resulting from mono-demetallation of **5** by dppe has previously been reported with a ³¹P NMR signal at 57 ppm (¹J_{RhP} = 134.2 Hz),[105] consistent with the NMR signature of **9** in the crude reaction mixture. The fact that one signal for **H_w** and **C_w** respectively was observed in the NMR spectra of **9** implies rapid ring slippage of the Rhᴵ(CO)₂ fragment across the pentalenide core in solution.

The above results show that although **5** does not react with mono- or bidentate pyridines, chelating phosphines readily bind to the Rhᴵ(CO)₂ centre to displace both carbonyls and lead to demetallation of the pentalenide. With monodentate phosphines progressive carbonyl substitution occurs on both Rhᴵ(CO)₂ centres which in the case of strong σ-donors can lead to a disproportionating demetallation reaction. Thus, ligand exchange reactions using less basic and more π-accepting phosphites[106] with lower steric demand in comparison to phosphines were tried next.

Phosphites. As seen before with PPh₃, the addition of one equivalent P(OPh)₃ to a solution of **5** in THF resulted in the desymmetrisation of the **Ph₄Pn²⁻** ligand with two new wingtip signals **H_wa** and **H_wb** appearing in the ¹H NMR at 6.22 ppm and 6.75 ppm, respectively, suggesting monosubstitution on one Rh centre of **5** to form [Rhᴵ(CO)₂;Rhᴵ(CO)(P{OPh}₃)][μ:η⁵:η⁵Ph₄Pn] (**10**). The two inequivalent wingtips could be distinguished by ¹H–³¹P-HMBC, with **H_Wa** at 6.22 ppm displaying a cross peak with the new ³¹P signal at 130.6 ppm. The difference in wingtip shift, Δw, of 0.53 ppm is similar to that observed with monosubstitution with PPh₃ in **6** (Δw = 0.48 ppm). Interestingly, while the magnitude of the Rh–P coupling in **10** was consistent with that reported for [CpRhᴵ(CO)(P{OPh}₃)] (¹J_{RhP} = 328.8 Hz), the ³¹P{H} shift of the asymmetrically twinned bimetallic was found 70 ppm downfield compared to the mononuclear complex (130.6 ppm *versus* 62.7 ppm).[94] When an excess of P(OPh)₃ was added to **5**, the ¹H NMR spectrum showed an increase in the symmetry of the aromatic region again, with a single **H_w** signal emerging at 5.90 ppm (1 ppm upfield of that of **5**) suggesting increased back-bonding from the metals to **Ph₄Pn²⁻**. These signatures were consistent with each Rhᴵ(CO)₂ fragment undergoing monosubstitution each to give the symmetrically di-substituted complex [Rhᴵ(CO)(P{OPh}₃)]₂[μ:η⁵:η⁵Ph₄Pn] (**11**) instead of forming inequivalent Rhᴵ(CO)₂ and Rhᴵ(P{OPh}₃)₂ moieties within the same complex. The ³¹P{¹H} NMR spectrum of **11** showed a major peak centred at 129.3 ppm (¹J_{RhP} = 342.7 Hz), close to the shift of **10** indicating an electronically similar
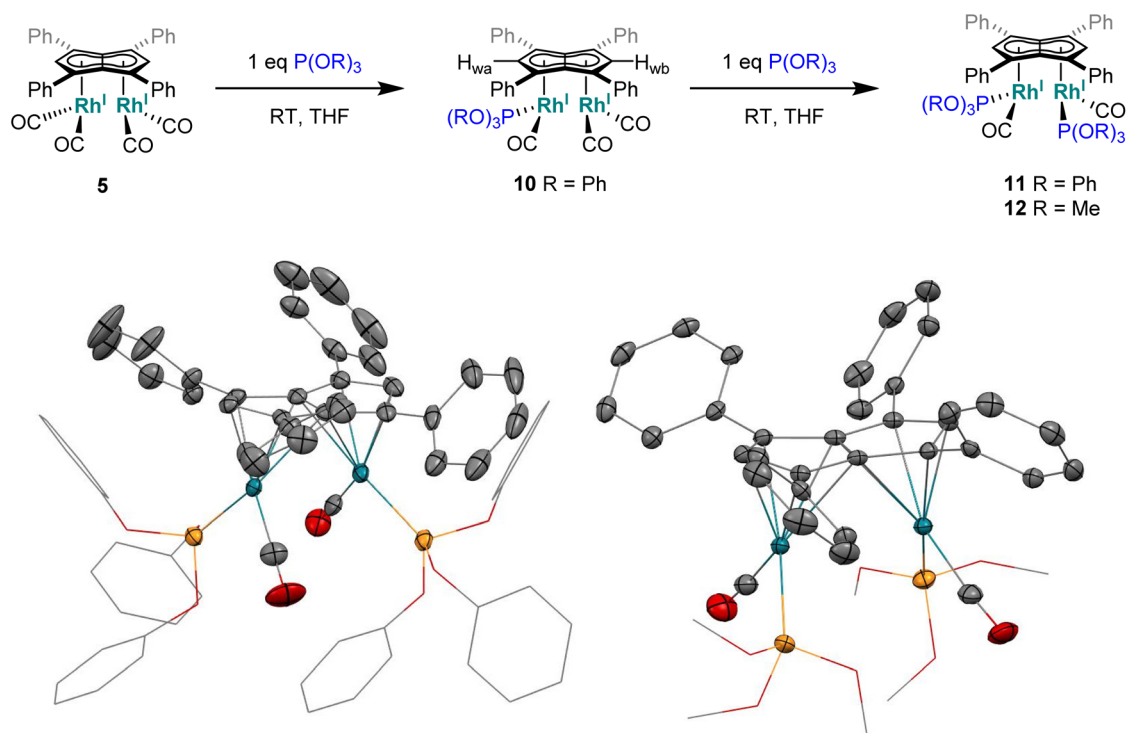

Fig. 9 Synthesis of *E-syn*-[Rhᴵ(CO)(P{OPh}₃)]₂[μ:η⁵:η⁵Ph₄Pn] (**11**) and *E-syn*-[Rhᴵ(CO)(P{OMe}₃)]₂[μ:η⁵:η⁵Ph₄Pn] (**12**) (top) and their X-ray crystal structure with thermal ellipsoids at the 50% probability level (bottom; hydrogen atoms omitted for clarity).

environment consistent with two $Rh^I(P\{OPh\}_3)(CO)$ moieties. When two equivalents of $P(OPh)_3$ were used a mixture of the mono- and bis-complexes **10** and **11** was observed, suggesting some (perhaps steric) barrier to forming the bis-product. With four or more equivalents of $P(OPh)_3$ clean formation of **11** was consistently observed, with no signs of demetallation unlike when using phosphines. X-ray crystallographic analysis of **11**, the first heteroleptic half-baguette pentalenide complex, confirmed retention of the *syn*-geometry of metal fragments with the phosphite ligands arranged in an *E*-geometry (Fig. 9). The Rh–Rh distance of 2.960 Å was slightly longer in **11** than in **5** (2.913 Å), leading to a FSR of 1.19, likely as a consequence of the increased steric crowding around each Rh(ɪ) centre. The Rh–C$_t$ distances were comparable to that of **5** (1.9969(12) Å and 2.0013(11) *versus* 1.997 Å) and the ring slippage values Δ were marginally lower (0.25 *versus* 0.27) revealing a slightly smaller degree of deviation towards η^3 than in **5**. The hinge angle of **11** showed that the C$_5$-rings deviated from planarity by an average of 8.5°, 1.7° less than in **5** whilst the angle between the L–Rh–L plane and Pn plane was 76.7°. The Rh–CO bond lengths were on average 0.03 Å shorter than in **5** suggesting an increase in Rh–CO back-bonding which was further supported by blueshifted CO bands at 1982 and 1961 cm^{-1} in the IR spectrum of **11** (*cf.* 1992, 2025, 2046 and 2064 cm^{-1} in **5**). The analogous reaction with $P(OMe)_3$ led to the formation of a variety of products, including a bis-substituted product, *E-syn*-[$Rh^I(CO)(P\{OMe\}_3)]_2[\mu:\eta^5:\eta^5Ph_4Pn]$ (**12**) which was found to be isostructural to **11** by single-crystal XRD exhibiting a ring slippage value of Δ = 0.27, a hinge angle of 9.5° and an angle of 78.2° between the L–Rh–L plane and the plane of Ph_4Pn^{2-}.

Conclusion

We have reported the synthesis of a series of bimetallic Rh(ɪ) half-baguette complexes from transmetalation of Ph_4Pn^{2-} salts with [$Rh^IL_2X]_2$ complexes. With either **Mg[Ph₄Pn]** or **Li·K [Ph₄Pn]** the same transmetalation product was obtained, consistent with the notion that in ethereal solution s-block pentalenides exist as solvent-separated ion pairs.[60,61] However, **Mg [Ph₄Pn]** provides practical advantages with cleaner formation of the transmetalation product and easy removal of $MgCl_2$ by induced precipitation of [$MgCl_2(dioxane)$]. **[Rh^I(COD)]₂[Ph₄Pn]** (**1**), **[Ir^I(COD)]₂[Ph₄Pn]** (**2**), **[Rh^I(NBD)]₂[Ph₄Pn]** (**3**) and **[Rh^I(C₂H₄)₂]₂[Ph₄Pn]** (**4**) all formed exclusively as linked *anti*-bimetallics, whilst the twinned *syn*-bimetallic **[Rh^I(CO)₂]₂[Ph₄Pn]** (**5**) was obtained regardless whether the monometallic [$Rh^I(acac)(CO)_2$] or bimetallic [$Rh^I(CO)_2(\mu$-Cl)]$_2$ precursors were used. DFT calculations revealed a mix of repulsive M–M and attractive ML$_2$–ML$_2$ interactions which weakly favour *syn* arrangement in the absence of steric clash between the auxiliary ligands L. Neither *anti*-**[Rh^I(NBD)]₂[Ph₄Pn]** nor *syn*-**[Rh^I(CO)₂]₂[Ph₄Pn]** displayed Lewis-basic reactivity towards $AlCl_3$ due to being surrounded by π-acceptor ligands in a distorted trigonal–bipyramidal 18-electron configuration.

Attempted ligand exchange reactions of *syn*-**[Rh^I(CO)₂]₂[Ph₄Pn]** with N-donor ligands were unsuccessful, whilst the introduction of strongly σ-donating and/or chelating phosphines led to rhodium abstraction from Ph_4Pn^{2-}. With PMe_3 this process was accompanied by disproportionation, forming Rh(0) dimers and the ion pair **[Rh^{II}(PMe₃)₄(CO)][Ph₄Pn]** (**8**). With dppe a single Rh(ɪ) centre was abstracted to yield the salt **[Rh^I(dppe)₂][Rh^I(CO)₂(η⁵Ph₄Pn)]** (**9**) featuring an anionic, mono-nuclear pentalenide complex which could serve as a synthon to access heterobimetallic complexes in the future. PPh_3 and $P(OPh)_3$ reacted similarly towards **5** to successively yield the monosubstituted complexes **[Rh^I(CO)₂;Rh^I(CO)(PPh₃)][Ph₄Pn]** (**6**) and **[Rh^I(CO)₂;Rh^I(CO)(P{OPh}₃)][Ph₄Pn]** (**10**) respectively. The di-substituted complexes *E-syn*-**[Rh^I(CO)(PPh₃)]₂[Ph₄Pn]** (**7**) and *E-syn*-**[Rh^I(CO)(P{OR}₃)]₂[Ph₄Pn]** (R = Ph **11**, R = Me **12**) could be accessed using stoichiometric amounts of PPh_3 and an excess of $P(OR)_3$ respectively. The latter were characterised by XRD which showed each rhodium centre underwent monosubstitution, with overall retention of the *syn*-geometry and the phosphite ligands adopting *E*-conformation due to sterics. These results will be useful in guiding the targeted derivatisation of future transition metal pentalenide complexes to test and exploit intermetallic cooperation in linked and twinned bimetallics. Related mono-metallic **Cp** complexes have been employed in a range of chemistries including C–H and Si–H activation[107] and cycloadditions[108–113] as well as synthons for heterometallic clusters,[114,115] offering a wealth of opportunities for bimetallic half-baguette pentalenide complexes.

Experimental

General considerations

All reactions were conducted under argon using standard Schlenk techniques or a MBraun Unilab Plus glovebox unless stated otherwise. All commercially available materials were purchased from Sigma Aldrich, Fisher or Acros.

Solvents

Methanol was dried and distilled over magnesium. Toluene was dried and distilled over sodium. THF, hexane and pentane were dried and distilled over potassium. C_6D_6 was distilled over CaH_2 and stored over 4 Å molecular sieves. TMEDA, DME and 1,4-dioxane were distilled over CaH_2.

Reagents

1,3,4,6-Tetraphenyl-1,2-dihydropentalene (Ph₄PnH₂),[60] Lithium potassium 1,3,4,6-tetraphenylpentalenide (Li·K[Ph₄Pn]),[60] Magnesium 1,3,4,6-tetraphenylpentalenide (Mg[Ph₄Pn]),[61] [$Rh^I(COD)(\mu$-Cl)]$_2$,[116] [$Ir^I(COD)(\mu$-Cl)]$_2$[117] and [$Rh^I(NBD)(\mu$-Cl)]$_2$[118] were prepared according to literature procedures. [$Rh^I(CO)_2(\mu$-Cl)]$_2$ and [$Rh^I(C_2H_4)_2(\mu$-Cl)]$_2$ were used as received.

Paper

Analysis

NMR spectra were obtained using either a 500 MHz Bruker Avance III, a 500 MHz Bruker Avance III HD with nitrogen cooled CryoProbe Prodigy (BBO) or a 400 MHz Bruker AvanceNeo with room temperature iProbe. Spectra were recorded at 25 °C unless stated otherwise. Chemical shifts (δ) are given in ppm and referenced to residual proton chemical shifts from the NMR solvent for ^{1}H and ^{13}C{^{1}H} spectra. UV-vis, NIR and IR spectroscopy were performed inside a MBraun Unilab Plus glovebox. UV-vis and NIR spectra were obtained using a fibre-optic AvaSpec-2048L photospectrometer (UV-vis) and an AvaSpec-NIR256 (NIR) with an AvaLight-DH-S-BAL light source and 400 μm cables (Avantes), data was collected between 250 nm and 1000 nm with an integration time of 4 ms (UV-vis) and between 910 nm and 1700 nm with an integration time of 0.26 ms (NIR). IR spectra were obtained using a Bruker Alpha II FT-IR (recorded between 4000 and 400 cm^{-1} with 24 scans at 2 cm^{-1} resolution).

Single X-ray diffraction analysis was carried out at the Material and Chemical Characterisation (MC^2) Facility at the University of Bath using a RIGAKU SuperNova Dual EoS2 single crystal diffractometer. Mass spectrometry was carried out at the Material and Chemical Characterisation Facility at the University of Bath using a Bruker MaXis HD ESI-QTOF with direct injection. Samples were prepared in THF inside an argon filled glovebox.

Synthesis of *anti*-[Rh^I(COD)]$_2$[μ:η^5:η^{5}Ph$_4$Pn] (1)

[Rh(COD)(μ-Cl)]$_2$ (16 mg, 0.03 mmol) was dissolved in 0.5 mL THF and added, by syringe, to a THF solution of **Mg[Ph$_4$Pn]** (20 mg, 0.03 mmol) in THF (0.5 ml). The reaction was stirred for one hour during which all solid dissolved and a colour change to red was observed. Then dioxane (0.3 mL) was added and the solution stirred for another hour, during which a creamy white precipitate formed. The supernatant was extracted *via* filtration and concentrated to 0.2 mL volume. To this, pentane (0.5 mL) was added, and the mixture stood overnight at −35 °C. The supernatant was removed, and the resultant red powder dried under vacuum for one hour to give the product (5 mg, 20%). Crystals suitable for XRD could be grown from standing of a THF solution at −35 °C.
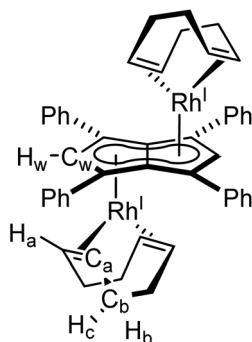

^{1}**H NMR** (500 MHz, C$_6$D$_6$) δ: 7.44 (d, $^3J_{HH}$ = 7.2 Hz, 8H, ArH), 7.13–7.09 (m, 11H, ArH), 6.10 (s, 2H, H$_w$), 3.92 (bs, 8H, H$_a$), 2.08 (bs, 9H, H$_c$/H$_b$), 1.77 (d, $^2J_{HH}$ = 7.9 Hz, 8H, H$_c$/H$_b$).

^{13}**C{^{1}H} NMR** (126 MHz, THF-H$_8$) δ: 136.2, 129.7, 128.1, 126.8, 99.3 (d, $^1J_{RhC}$ = 4.8 Hz, C$_w$), 91.2 (d, $^1J_{RhC}$ = 4.3 Hz), 89.9, 72.9 (d, $^1J_{RhC}$ = 13.6 Hz, C$_a$), 32.3 (C$_b$).

HR APCI-MS (+) *m/z* expected for [M + H] = 829.1782, found 829.1722

Synthesis of *anti*-[Ir^I(COD)]$_2$[μ:η^5:η^{5}Ph$_4$Pn] (2)

[Ir(COD)(μ-Cl)]$_2$ (20 mg, 0.03 mmol) was dissolved in 0.5 mL THF and added, by syringe, to a THF solution of Mg[Ph$_4$Pn] (20 mg, 0.03 mmol) in THF (0.5 ml). The reaction was stirred for one hour during which all solid dissolved and a colour change to red was observed. Then dioxane (0.3 mL) was added and the solution stirred for another hour, during which a creamy white precipitate formed. The supernatant was extracted *via* filtration and concentrated to 0.2 mL volume. To this, pentane (0.5 mL) was added, and the solution stood overnight at −35 °C. The supernatant was removed, and the resultant yellow powder dried under vacuum for one hour to give the product (12 mg, 39%). Crystals suitable for XRD could be grown from standing of a THF solution at −35 °C.
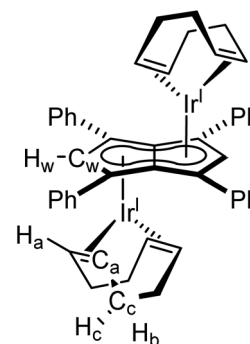
^{1}**H NMR** (500 MHz, C$_6$D$_6$) δ: 7.32–7.31 (m, 8H, ArH), 7.10–7.09 (m, 12H, ArH), 6.10 (s, 2H, H$_w$), 3.98 (bs, 8H, H$_a$), 2.00–1.98 (m, 9H, H$_c$/H$_b$), 1.74–1.72 (m, 8H, H$_c$/H$_b$)

^{13}**C{^{1}H} NMR** (126 MHz, THF-H$_8$) δ: 134.9, 130.2, 128.3, 127.2, 92.3 (C$_w$), 86.9, 86.3, 56.1 (C$_a$), 33.4 (C$_b$)

HR APCI-MS (+) *m/z* expected for [M + H] = 1009.2931, found 1009.2829

Synthesis of *anti*-[Rh^I(NBD)]$_2$[μ:η^5:η^{5}Ph$_4$Pn] (3)

Mg[Ph$_4$Pn] (20 mg, 0.03 mmol) was dissolved in THF (0.5 mL) and to this solution [Rh(NBD)(μ-Cl)]$_2$ (14 mg, 0.03 mmol) in THF (0.5 mL) was added dropwise and stirred. Upon addition, complete dissolution of all solid was observed and a colour change to dark yellow was seen. The reaction was stirred for one hour during which a yellow precipitate formed. The precipitate was collected *via* filtration over a silica frit and washed with hexane (2 × 1 mL) and dried to afford the product as a yellow/orange powder (18 mg, 76%). Crystals suitable for XRD

could be grown from standing of a THF solution at −35 °C.
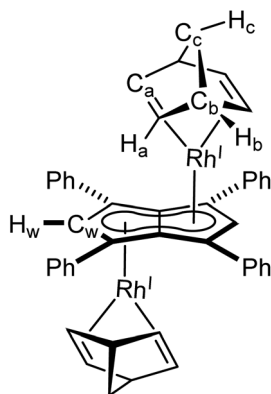
^{1}**H NMR** (500 MHz, C$_6$D$_6$) δ: 7.35–7.33 (m, 9H, ArH), 7.07–7.06 (m, 13H ArH), 6.22 (d, $^2J_{RhH}$ = 0.8 Hz, 2H, H$_w$), 3.4–3.32 (m, 8H, H$_a$), 3.17 (bs, 5H, H$_b$), 0.81 (s, 4H, H$_c$).

^{13}**C{^{1}H} NMR**: (126 MHz, C$_6$D$_6$) δ: 136.8, 129.5, 128.4, 126.3, 97.4 (d, $^1J_{RhC}$ = 5.8 Hz, C$_w$), 88.8 (d, $^1J_{RhC}$ = 4.3 Hz), 88.1, 58.1 (d, $^3J_{RhC}$ = 7 Hz, C$_c$), 48.5 (C$_b$), 41.3 (d, $^1J_{RhC}$ = 10.3 Hz, C$_a$).

HR APCI-MS (+) m/z expected for [M + H] = 797.1156, found 797.1205.

Synthesis of [Rh^I(C$_2$H$_4$)$_2$]$_2$[μ:η^5:η^{5}Ph$_4$Pn] (4)

Mg[Ph$_4$Pn] (20 mg, 0.03 mmol) was dissolved in THF (0.5 mL) and to this solution [Rh(C$_2$H$_4$)$_2$(μ-Cl)]$_2$ (12 mg, 0.03 mmol) in THF (0.5 mL) was added. An immediate colour change from orange to dark green was observed. Full conversion as determined by ^{1}H NMR spectroscopy. Crystals suitable for XRD could be grown from standing of a THF solution at −35 °C, after treatment with dioxane to remove MgCl$_2$ by-product. Due to the instability of this complex, it could not be cleanly isolated to obtain a yield.
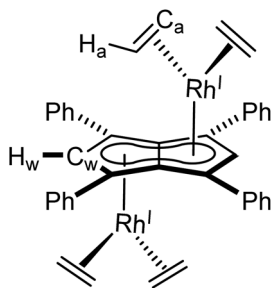
^{1}**H NMR** (500 MHz, C$_6$D$_6$) δ: 7.41–7.39 (m, 8H, Ar–H), 7.10–7.09 (m, 12H, Ar–H), 5.98 (d, $^2J_{RhH}$ = 0.7 Hz, 2H, H$_w$), 2.19 (d, $^2J_{RhH}$ = 1.8 Hz, 16H, H$_a$).

^{13}**C{^{1}H} NMR**: (126 MHz, C$_6$D$_6$) δ: 134.8, 130.8, 129.8, 127.2, 98.6 (d, $^1J_{RhC}$ = 5.2 Hz, C$_w$), 91.8 (d, $^1J_{RhC}$ = 4.3 Hz), 89.5, 50.4 (d, $^1J_{RhC}$ = 14.2 Hz, C$_a$).

Synthesis of syn-[Rh^I(CO)$_2$]$_2$[μ:η^5:η^{5}Ph$_4$Pn] (5)

Method A: [Rh(CO)$_2$(μ-Cl)]$_2$ (12 mg, 0.03 mmol) was dissolved in THF (1 mL) and added dropwise to a solution of Mg[Ph$_4$Pn] (20 mg, 0.03 mmol) in THF (0.5 mL) and stirred. A colour change from orange to dark yellow was observed along with

complete dissolution of Mg[Ph$_4$Pn]. The reaction was allowed to stir for one hour, after dioxane (0.3 mL) was added and the reaction stirred for a further hour during which a brown precipitate formed. The supernatant was collected *via* filtration and concentrated to ∼0.3 mL. To this pentane (0.5 mL) was added and the solution stood overnight at −35 °C. The supernatant was decanted off and the powder dried under vacuum to give the product (7 mg, 32%). Crystals suitable for XRD could be grown from standing of a THF/pentane solution (2 : 1) at −35 °C.

Method B: [Rh(acac)(CO)$_2$] (8 mg, 0.031 mmol) was dissolved in THF (0.5 mL) and added dropwise to a solution of Mg[Ph$_4$Pn] (10 mg, 0.015 mmol) in THF (0.5 mL). A colour change from orange to dark yellow was observed alongside complete dissolution of Mg[Ph$_4$Pn]. Formation of the product was confirmed *in situ* by ^{1}H NMR.

Method C: Li·K[Ph$_4$Pn] (0.05 mmol) was generated *in situ* and to this a solution of [Rh(CO)$_2$(μ-Cl)]$_2$ (29 mg, 0.07 mmol) in THF (0.5 mL) was added dropwise. A colour change from red to dark yellow was observed and the product identified *in situ* by ^{1}H NMR.

Method D: Li·K[Ph$_4$Pn] (0.05 mmol) was generated *in situ* and to this a solution of [Rh(acac)(CO)$_2$] (51 mg, 0.2 mmol) in THF (0.5 mL) was added dropwise. A colour change from red to dark yellow was observed and the product identified *in situ* by ^{1}H NMR.

Method E: [Mg^{n}Bu(THF)$_2$][Ph$_4$Pn] (10 mg, 0.012 mmol) was dissolved in C$_6$D$_6$ (0.5 mL) and to this a solution of [Rh(CO)$_2$(μ-Cl)]$_2$ (5 mg, 0.012 mmol) in C$_6$D$_6$ (0.5 mL) was added slowly. A colour change from bright yellow to dark yellow was observed and the product identified *in situ* by ^{1}H NMR.
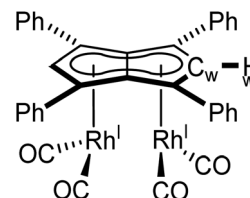
^{1}**H NMR** (500 MHz, THF-H$_8$) δ: 7.16 (d, $^3J_{HH}$ = 7.1 Hz, 8H, ArH), 7.12 (d, $^3J_{HH}$ = 7.3 Hz, 3H, ArH), 7.04 (t, $^3J_{HH}$ = 7.7 Hz, 8H, ArH), 6.91 (d, $^2J_{RhH}$ = 1.4 Hz, 2H, H$_w$).

^{13}**C{^{1}H} NMR** (126 MHz, THF-H$_8$) δ: 194.5 (d, $^1J_{RhC}$ = 83.8 Hz, CO), 133.7, 130.5, 128.2, 128.2, 112.1, 90.1 (d, $^1J_{RhC}$ = 7.0 Hz, C$_w$), 81.9 (d, $^1J_{RhC}$ = 4.3 Hz).

HR APCI-MS (+) m/z expected for [M + H] = 724.9706, found = 724.9677.

IR (ν_{CO}, cm^{-1}): 2064, 2046, 2025, 1992.

General procedure for ligand substitution reactions

5 was generated *in situ* by the addition of [Rh(CO)$_2$(μ-Cl)]$_2$ (12 mg, 0.03 mmol in 0.3 mL THF) to Mg[Ph$_4$Pn] (20 mg, 0.03 mmol in 0.5 mL THF) with formation confirmed by ^{1}H NMR. An appropriate amount of ligand was then added (0.03 mmol, 0.06 mmol, or 0.12 mmol). Solid ligands were added as a THF solution (0.3 mL) and liquids were added

directly to the solution of **5**, before dioxane (0.2 mL) was added, and the solution left to stand for 10 minutes after which it was syringe filtered to remove the precipitated [MgCl$_2$(dioxane)]$_\infty$. In the cases of **6**, **7**, **8** and **10** the products could not be cleanly isolated and were identified *in situ* using multi-nuclear 1D and 2D NMR techniques supported by mass spectrometry. The original NMR spectra can be found in Fig. S28–S47.†

syn-[Rh^I(CO)$_2$;Rh^I(CO)(PPh$_3$)][μ:η^5:η^{5}Ph$_4$Pn] (6)
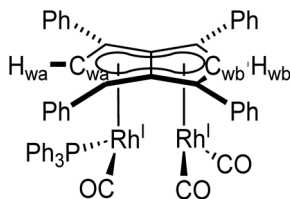
^{1}H NMR (500 MHz, THF-H$_8$) δ: 6.71 (s, 1H, H$_{wb}$), 6.23 (s, 1H, H$_{wa}$).

^{13}C{^{1}H} NMR (126 MHz, THF-H$_8$) δ: 195.2 (dd, $^1J_{RhC}$ = 84.3 Hz, $^2J_{CP}$ = 3.3 Hz, CO), 93.4 (C$_{wa}$), 88.7 (d, $^1J_{RhC}$ = 6.5 Hz, C$_{wb}$).

^{31}P{^{1}H} NMR (202 MHz, THF-H$_8$) δ: 48.1 ppm ($^1J_{RhP}$ = 202 Hz).

HR ESI-MS (+) *m/z* expected for [M − Rh(CO)$_2$] = 799.1632, found = 799.1622.

syn-[Rh^I(CO)(PPh$_3$)]$_2$[μ:η^5:η^{5}Ph$_4$Pn] (7)
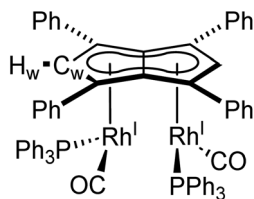
^{31}P{^{1}H} NMR (202 MHz, THF-H$_8$) δ: 51.4 ($^1J_{RhP}$ = 198 Hz).

HR ESI-MS (+) *m/z* expected for [M] = 1192.1547, found = 1192.1459; *m/z* expected for [M − Rh(CO)(PPh$_3$)] = 799.1632, found = 799.1590.

[Rh^{II}(PMe$_3$)$_4$(CO)][Ph$_4$Pn] (8)

As per the general procedure, PMe$_3$ (0.12 mmol, 1M in THF) was added to a THF solution of **5**. A colour change to dark red was observed. To this solution dioxane (0.2 mL) was added and subsequently filtered. Addition of pentane (1 mL, 1 : 1 ratio with THF) followed by standing of the solution at −35 °C yielded dark red crystals of *[Rh^{II}(PMe$_3$)$_4$(CO)][Ph$_4$Pn]* suitable for X-ray diffraction. Due to the instability of this complex, it could not be cleanly isolated to obtain a yield.
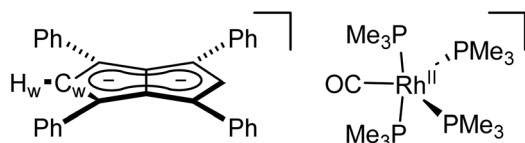
^{31}P{^{1}H} NMR (202 MHz, THF-H$_8$) δ: −16.2 (bs), −34.4 (bs).

HR APCI-MS (−) *m/z* expected for [M − Rh(CO)(PMe$_3$)$_4$] = 406.1722, found = 406.1769.

[Rh^I(dppe)$_2$][Rh^I(CO)$_2$(η^{5}Ph$_4$Pn)] (9)
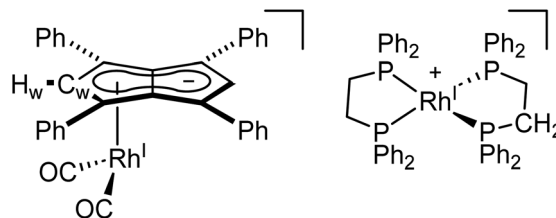
The crude reaction mixture was concentrated to *circa* 0.3 mL, 1 mL hexane added and the solution stood at −35 °C for one hour. The supernatant was removed and the solid dried under vacuum to afford the product (20.3 mg, 45%).

^{1}H NMR (500 MHz, THF-H$_8$) δ: 7.29 (t, $^3J_{HH}$ = 7 Hz, 6H, ArH), 7.18–7.11 (m, 36H, ArH), 7.04 (t, $^3J_{HH}$ = 7.6 Hz, 8H, ArH), 6.91 (d, $^2J_{RhH}$ = 0.9 Hz, 2H, H$_w$), 2.11 (bs, CH$_2$).
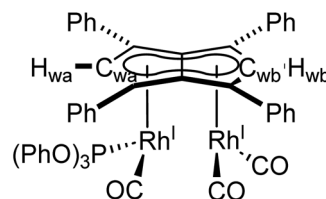
^{13}C{^{1}H} NMR (126 MHz, THF-H$_8$) δ: 194.4 (d, $^1J_{RhH}$ = 82.8 Hz, CO), 134.0, 133.6, 131.3, 130.5, 129.4, 129.0, 128.9, 128.5, 128.2, 128.1, 121.1, 90.1 (d, $^1J_{RhC}$ = 7.1 Hz, C$_w$), 81.9 (d, $^1J_{RhC}$ = 4.4 Hz), 42.1 Hz (CH$_2$).

^{31}P{^{1}H} NMR (202 MHz, THF-H$_8$) δ: 57.6 (d, $^1J_{RhP}$ = 128 Hz).

HR ESI-MS (+) *m/z* expected for [M − Rh(CO)$_2$(Ph$_4$Pn)] = 899.1756, found = 899.1715.

IR (ν_{CO}, cm^{-1}): 1980, 1918.

syn-[Rh^I(CO)$_2$;Rh^I(CO)(P{OPh}$_3$)][μ:η^5:η^{5}Ph$_4$Pn] (10)

^{1}H NMR (500 MHz, THF-H$_8$) δ: 6.75 (s, 1H, H$_b$), 6.22 (s, 1H, H$_a$).

^{13}C{^{1}H} NMR (126 MHz, THF-H$_8$) δ: 88.6 (d, $^1J_{RhC}$ = 7.4 Hz, H$_{wb}$), 81.9 (d, $^1J_{RhC}$ = 4.5 Hz, H$_{wa}$).

^{31}P{^{1}H} NMR (202 MHz, THF-H$_8$) δ: 130.6 (d, $^1J_{RhP}$ = 328 Hz).

E-syn-[Rh^I(CO)(P{OPh}$_3$)]$_2$[μ:η^5:η^{5}Ph$_4$Pn] (11)
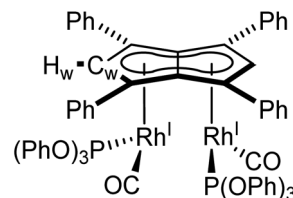
Using 0.12 mmol P(OPh)$_3$. Hexane (1 mL) was added to the crude reaction mixture, and the solution stood overnight at −35 °C. The supernatant was removed, and the resultant

brown powder dried under vacuum for 2 hours to give the product (16.4 mg, 41%).

^{1}H NMR (500 MHz, THF-H$_8$) δ: 7.18–7.15 (m, 13H, ArH), 7.05–6.99 (m, 19H, ArH), 6.91–6.87 (m, 16H, ArH), 5.90 (s, 2H, H$_w$).

^{13}C{^{1}H} NMR (126 MHz, THF-H$_8$) δ: 152.8 (d, $^{1}J_{RhC}$ = 10.5 Hz), 135.4, 130.9, 129.7, 127.6, 126.7, 124.7, 122.4 ($^{1}J_{RhC}$ = 3.8 Hz), 109.6, 89.1 (m, C$_w$), 81.0 [CO not resolved].

^{31}P{^{1}H} NMR (202 MHz, THF-H$_8$) δ: 128.5 (d, $^{1}J_{RhP}$ = 344 Hz).
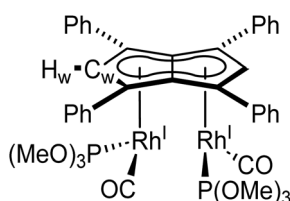
HR ESI-MS (+) m/z expected for [M − Rh(CO)(P{OPh}$_3$)] = 847.1479, found = 847.1561.

IR (ν_{CO}, cm^{-1}): 1982, 1961.

E-syn-[Rh^{I}(CO)(P{OMe}$_3$)]$_2$[μ:η^5:η^{5}Ph$_4$Pn] (12)

Using 0.06 mmol P(OMe)$_3$. The solvent was removed under vacuum and the resultant brown solid washed with *n*-hexane (3 × 0.5 mL) to afford the product (21.4 mg, 74%).

^{1}H NMR (500 MHz, THF-H$_8$) δ: 7.20 (d, $^{3}J_{HH}$ = 7 Hz, 8H, ArH), 6.99–6.93 (m, 12H, ArH), 6.64 (s, 2H, H$_w$) [methyl groups obscured by solvent].

^{13}C{^{1}H} NMR (126 MHz, THF-H$_8$) δ: 136.5, 130.7, 127.3, 126.2, 110.1, 88.3 ($^{1}J_{RhC}$ = 7 Hz, C$_w$), 80.1 (dd, $^{1}J_{RhC}$ = 10 Hz, $^{2}J_{PC}$ = 4 Hz), 52.2 (d, $^{2}J_{RhC}$ = 3 Hz, CH$_3$).

^{31}P{^{1}H} NMR (202 MHz, THF-H$_8$) δ: 146.2 (d, $^{1}J_{RhP}$ = 309 Hz).

HR ESI-MS (+) m/z expected for [M] = 916.0303, found = 916.0284.

Conflicts of interest

There are no conflicts of interest to declare.

Acknowledgements

References

1 J. Campos, Bimetallic cooperation across the periodic table, *Nat. Rev. Chem.*, 2020, **4**, 696–702.

2 C. M. Farley and C. Uyeda, Organic Reactions Enabled by Catalytically Active Metal–Metal Bonds, *Trends Chem.*, 2019, **1**, 497–509.

3 J. F. Berry and C. M. Thomas, Multimetallic complexes: synthesis and applications, *Dalton Trans.*, 2017, **46**, 5472.

4 J. M. Gil-Negrete and E. Hevia, Main group bimetallic partnerships for cooperative catalysis, *Chem. Sci.*, 2021, **12**, 1982–1992.

5 R. H. Lam, S. T. Keaveney, B. A. Messerle and I. Pernik, Bimetallic Rhodium Complexes: Precatalyst Activation-Triggered Bimetallic Enhancement for the Hydrosilylation Transformation, *ACS Catal.*, 2023, **13**, 1999–2010.

6 M. S. Jeletic, I. Ghiviriga, K. A. Abboud and A. S. Veige, Mono- and bimetallic rhodium(I) complexes supported by new C$_2$-symmetric bis-N-heterocyclic carbene ligands: Metalation via C=C bond cleavage under mild conditions, *Organometallics*, 2007, **26**, 5267–5270.

7 F. Min, N. D. Jones, K. Friesen, L. Guanyang, M. J. Ferguson, R. McDonald, R. Lukowski and R. G. Cavell, Bimetallic, spirocyclic, methylene-bridged carbene complexes of rhodium and palladium derived by stepwise metalations of lithiated bis(diphenylphosphoranotrimethylsilylimido)methandiide, *Organometallics*, 2009, **28**, 1652–1665.

8 L. A. Oro, D. Carmona and J. Reedijk, Dinuclear rhodium (I) compounds containing diolefins and the 1,6-bis(2′-benzimidazolyl)-2,5-dithiahexane ligand, *Inorg. Chim. Acta*, 1983, **71**, 115–118.

9 C. Tan, H. Tinnermann, V. Wee, S. Tan, S. Sung, Q. Wang and R. D. Young, Synthesis of bimetallic rhodium phosphinine complexes with enhanced catalytic activity towards alkyne hydrosilylation, *J. Organomet. Chem.*, 2023, **986**, 122617.

10 T. A. Koizumi, Y. Ohkura and E. Tsuda, Synthesis, structure, and electrochemical behavior of a new dinuclear Rh(III) complex bridged by a bpp− ligand (bpp− = 3,5-bis(2-pyridyl) pyrazolate), *Inorg. Chem. Commun.*, 2016, **67**, 25–28.

11 M. Mintert and W. S. Sheldrick, Dinuclear Rh(I,I) and Rh (II,II) complexes containing bridging asymmetrically 2,7-disubstituted naphthyridines, *Inorg. Chim. Acta*, 1997, **254**, 93–98.

12 C. M. Thomas, A. Neels, H. Stoeckli-Evans and G. Süss-Fink, Rhodium-Catalysed Carbonylation of Methanol Using a New Multifunctional Ligand Isolation and Structural Characterisation of the Macrocycle [Rh$_2$I$_6$(CO)$_2$(C$_6$H$_4$N$_3$CH$_2$CO$_2$C$_4$H$_2$SCO$_2$CH$_2$C$_6$H$_4$N$_3$)]$_2$, *Eur. J. Inorg. Chem.*, 2001, 3005–3008.

13 M. E. Broussard, B. Juma, S. G. Train, W. J. Peng, S. A. Laneman and G. G. Stanley, A Bimetallic Hydroformylation Catalyst: High Regioselectivity and Reactivity Through Homobimetallic Cooperativity, *Science*, 1993, **260**, 1784–1788.

14 J. H. H. Ho, S. W. S. Choy, S. A. MacGregor and B. A. Messerle, Cooperativity in bimetallic dihydroalkoxylation catalysts built on aromatic scaffolds: Significant rate enhancements with a rigid anthracene scaffold, *Organometallics*, 2011, **30**, 5978–5984.

15 S. W. S. Choy, M. J. Page, M. Bhadbhade and B. A. Messerle, Cooperative catalysis: Large rate enhancements with bimetallic rhodium complexes, *Organometallics*, 2013, **32**, 4726–4729.

16 M. Maekawa, K. Sugimoto, T. Kuroda-Sowa, Y. Suenaga and M. Munakata, Syntheses and structures of dinuclear rhodium(I) complexes and 1-D zigzag-chain rhodium(I) co-ordination polymers bridged by rod-like bidentate nitrogen ligands, *J. Chem. Soc., Dalton Trans.*, 1999, 4357–4362.

17 T. Nakajima, M. Maeda, A. Matsui, M. Nishigaki, M. Kotani and T. Tanase, Unsymmetric Dinuclear Rh^I_2 and $Rh^I Rh^{III}$ Complexes Supported by Tetraphosphine Ligands and Their Reactivity of Oxidative Protonation and Reductive Dechlorination, *Inorg. Chem.*, 2022, **61**, 1102–1117.

18 K. Masada, K. Okabe, S. Kusumoto and K. Nozaki, A dinuclear Rh(−I)/Rh(I) complex bridged by biphilic phosphinine ligands, *Chem. Sci.*, 2023, **14**, 8524–8530.

19 L. J. Watson and A. F. Hill, C–H activation in bimetallic rhodium complexes to afford N-heterocyclic carbene pincer complexes, *Dalton Trans.*, 2023, **52**, 2164–2174.

20 S. Sun, C. A. Dullaghan, G. B. Carpenter, A. L. Rieger, P. H. Rieger and D. A. Sweigart, Synthesis and Structure of Bimetallic η^4,η^6-Naphthalene Complexes Containing a Mn-Mn Moiety Bonded in a syn-Facial Manner: A General Route to Homo- and Heteronuclear Bimetallic Complexes of Polyarenes, *Angew. Chem., Int. Ed. Engl.*, 1995, **34**, 2540–2542.

21 J. A. Reingold, K. L. Virkaitis, G. B. Carpenter, S. Sun, D. A. Sweigart, P. T. Czech and K. R. Overly, Chemical and electrochemical reduction of polyarene manganese tricarbonyl cations: Hapticity changes and generation of Syn- and Anti-facial bimetallic η^4,η^6-naphthalene complexes, *J. Am. Chem. Soc.*, 2005, **127**, 11146–11158.

22 K. D. Demadis, C. M. Hartshorn and T. J. Meyer, The Localized-to-Delocalized Transition in Mixed-Valence Chemistry, *Chem. Rev.*, 2001, **101**, 2655–2685.

23 W. Kaim, Concepts for metal complex chromophores absorbing in the near infrared, *Coord. Chem. Rev.*, 2011, **255**, 2503–2513.

24 P. Jutzi and N. Burford, Structurally Diverse π-Cyclopentadienyl Complexes of the Main Group Elements, *Chem. Rev.*, 1999, **99**, 969–990.

25 S. Bendjaballah, S. Kahlal, K. Costuas, E. Bévillon and J. Y. Saillard, The Versatility of Pentalene Coordination to Transition Metals: A Density Functional Theory Investigation, *Chem. – Eur. J.*, 2006, **12**, 2048–2065.

26 O. T. Summerscales and F. G. N. Cloke, The organometallic chemistry of pentalene, *Coord. Chem. Rev.*, 2006, **250**, 1122–1140.

27 F. G. N. Cloke, J. C. Green, A. F. R. Kilpatrick and D. O'Hare, Bonding in pentalene complexes and their recent applications, *Coord. Chem. Rev.*, 2017, **344**, 238–262.

28 Y. A. Ustynyuk, A. K. Shestakova, V. A. Chertkov, N. N. Zemlyansky, I. V. Borisova, A. I. Gusev, E. B. Tchuklanova and E. A. Chernyshev, Synthesis, structure and fluxional behaviour of isomeric bis(trimethylstannyl)dihydropentalenes, *J. Organomet. Chem.*, 1987, **335**, 43–57.

29 F. G. N. Cloke, M. C. Kuchta, R. M. Harker, P. B. Hitchcock and J. S. Parry, Trialkylsilyl-substituted pentalene ligands, *Organometallics*, 2000, **19**, 5795–5798.

30 R. T. Cooper, F. M. Chadwick, A. E. Ashley and D. O'Hare, Synthesis and Characterization of Group 4 Permethylpentalene Dichloride Complexes, *Organometallics*, 2013, **32**, 2228–2233.

31 A. F. R. Kilpatrick, J. C. Green, F. Geoffrey, N. Cloke and N. Tsoureas, Bis(pentalene)di-titanium: a bent double-sandwich complex with a very short Ti-Ti bond, *Chem. Commun.*, 2013, **49**, 9434.

32 G. Balazs, F. G. N. Cloke, L. Gagliardi, J. C. Green, A. Harrison, P. B. Hitchcock, A. R. M. Shahi and O. T. Summerscales, A dichromium(II) bis(η^8-pentalene) double-sandwich complex with a spin equilibrium: Synthetic, structural, magnetic, and theoretical studies, *Organometallics*, 2008, **27**, 2013–2020.

33 A. E. Ashley, R. T. Cooper, G. G. Wildgoose, J. C. Green and D. O'Hare, Homoleptic Permethylpentalene Complexes: 'Double Metallocenes' of the First-Row Transition Metals, *J. Am. Chem. Soc.*, 2008, **130**, 15662–15677.

34 S. C. Binding, J. C. Green, W. K. Myers and D. O'Hare, Synthesis, Structure, and Bonding for Bis(permethylpentalene)diiron, *Inorg. Chem.*, 2015, **54**, 11935–11940.

35 G. Balazs, F. G. N. Cloke, A. Harrison, P. B. Hitchcock, J. Green and O. T. Summerscales, Mn_2 bis(pentalene): A mixed-spin bimetallic with two extremes of bonding within the same molecule, *Chem. Commun.*, 2007, 873–875.

36 O. T. Summerscales, C. J. Rivers, M. J. Taylor, P. B. Hitchcock, J. C. Green and F. G. N. Cloke, Double-sandwich pentalene complexes M_2(pent†)$_2$ (M = Rh, Pd; Pent† = 1,4-Bis(triisopropylsilyl) pentalene): Synthesis, structure, and bonding, *Organometallics*, 2012, **31**, 8613–8617.

37 S. C. Jones, T. Hascall, S. Barlow and D. O'Hare, Pentalene Complexes of Group 7 Metal Carbonyls: An Organometallic Mixed-Valence System with Very Large Metal-Metal Electronic Coupling, *J. Am. Chem. Soc.*, 2002, **124**, 11610–11611.

38 S. C. Jones, P. Roussel, T. Hascall and D. O'Hare, Convenient solution route to alkylated pentalene ligands: New metal monoalkylpentalenyl complexes, *Organometallics*, 2006, **25**, 221–229.

39 D. F. Hunt and J. W. Russell, Phenylpentalenediiron pentacarbonyl, *J. Organomet. Chem.*, 1972, **46**, C22–C24.

40 D. F. Hunt and J. W. Russell, A Stable Transition Metal π Complex of Dimethylaminopentalene, *J. Am. Chem. Soc.*, 1972, **94**, 7198–7199.

41 W. Weidemüller and K. Hafner, Synthesis of Carbonyliron Complexes of Pentalene and Its Derivatives, *Angew. Chem., Int. Ed. Engl.*, 1973, **12**, 925–925.

42 D. F. Hunt and J. W. Russell, Iron carbonyl complexes of pentalene and dihydropentalene, *J. Organomet. Chem.*, 1976, **104**, 373–376.

43 A. E. Ashley, G. Balázs, A. R. Cowley, J. C. Green and D. O'Hare, syn-Permethylpentalene Iron and Cobalt Carbonyl Complexes: Proximity Bimetallics Lacking Metal-Metal Bonding, *Organometallics*, 2007, **26**, 5517–5521.

44 A. Miyake and A. Kanai, Allyldihydropentalenylene Complexes of Transition Metals, *Angew. Chem., Int. Ed. Engl.*, 1971, **10**, 801–802.

45 S. A. R. Knox, F. Gordon and A. Stone, Approaches to the Synthesis of Pentalene via Metal Complexes, *Acc. Chem. Res.*, 1974, **7**, 321–328.

46 J. A. K. Howard, S. A. R. Knox, F. G. A. Stone, A. C. Szary and P. Woodward, Pentalene complexes from cyclo-octatrienes: Crystal structure of η,-(1,5-bistrimethylsilyl)pentalene-1,1,2,2,3,3,3,3-octacarbonyl-triangulo- triruthenium, $\{Ru_3(CO)_8[C_8H_4(SiMe_3)_2]\}$, *J. Chem. Soc., Chem. Commun.*, 1974, 788–789.

47 F. M. Chadwick, A. E. Ashley, R. T. Cooper, L. A. Bennett, J. C. Green and D. M. O'Hare, Group 9 bimetallic carbonyl permethylpentalene complexes, *Dalton Trans.*, 2015, **44**, 20147–20153.

48 A. F. R. Kilpatrick and F. G. N. Cloke, Reductive deoxygenation of CO_2 by a bimetallic titanium bis(pentalene) complex, *Chem. Commun.*, 2014, **50**, 2769–2771.

49 A. F. R. Kilpatrick, J. C. Green and F. G. N. Cloke, The Reductive Activation of CO_2 Across a Ti=Ti Double Bond: Synthetic, Structural, and Mechanistic Studies, *Organometallics*, 2015, **34**, 4816–4829.

50 N. Tsoureas, J. C. Green and F. G. N. Cloke, C-H and H-H activation at a di-titanium centre, *Chem. Commun.*, 2017, **53**, 13117–13120.

51 N. Tsoureas, J. C. Green and F. G. N. Cloke, Bis(pentalene) dititanium chemistry: C-H, C-X and H-H bond activation, *Dalton Trans.*, 2018, **47**, 14531–14539.

52 R. T. Cooper, F. M. Chadwick, A. E. Ashley and D. O'Hare, Double CO_2 activation by 14-electron η^8-permethylpentalene titanium dialkyl complexes, *Chem. Commun.*, 2015, **51**, 11856–11859.

53 F. M. Chadwick, R. T. Cooper and D. O'Hare, Zirconium and Hafnium Permethylpentalene Compounds, *Organometallics*, 2016, **35**, 2092–2100.

54 E. A. Hamilton, A. F. R. Kilpatrick, Z. R. Turner, D. A. X. Fraser, J. C. Buffet and D. O'Hare, CO_2 activation by permethylpentalene amido zirconium complexes, *Dalton Trans.*, 2021, **50**, 4494–4498.

55 K. Jonas, P. Kolb, G. Kollbach, B. Gabor, R. Mynott, K. Angermund, O. Heinemann and C. Kruger, Mononuclear Pentalene and Methylpentalene Complexes

56 F. M. Chadwick, R. T. Cooper, A. E. Ashley, J. C. Buffet and D. M. O'Hare, Early transition metal permethylpentalene complexes for the polymerization of ethylene, *Organometallics*, 2014, **33**, 3775–3785.

57 D. A. X. Fraser, Z. R. Turner, J. C. Buffet and D. O'Hare, Titanium and Zirconium Permethylpentalene Complexes, Pn*MCpRX, as Ethylene Polymerization Catalysts, *Organometallics*, 2016, **35**, 2664–2674.

58 F. Burgos, I. Chá Vez, J. M. Manriquez, M. Valderrama, E. Lago, E. Molins, F. Delpech, A. Castel and P. Riviè, A New Heterobimetallic Ru,Rh Complex with a Dianionic Pentalene as Bridging Ligand. Synthesis, Crystal Structure, and Catalytic Activity of $[Cp*Ru(\mu,\eta^5,\eta^3\text{-}C_8H_6)$ $Rh(\eta^4\text{-}COD)]$, *Organometallics*, 2001, **20**, 1287–1291.

59 N. A. Jenek, M. Balschun, S. M. Boyt and U. Hintermair, Connect Four: Tetraarylated Dihydropentalenes and Triarylated Monocyclic Pentafulvenes from Cyclopentadienes and Enones, *J. Org. Chem.*, 2022, **87**, 13790–13802.

60 S. M. Boyt, N. A. Jenek, H. J. Sanderson, G. Kociok-Köhn and U. Hintermair, Synthesis of a Tetraphenyl-Substituted Dihydropentalene and Its Alkali Metal Hydropentalenide and Pentalenide Complexes, *Organometallics*, 2022, **41**, 211–225.

61 H. J. Sanderson, G. Kociok-Köhn and U. Hintermair, Synthesis, Structure, and Reactivity of Magnesium Pentalenides, *Inorg. Chem.*, 2023, **62**, 15983–15991.

62 F. G. N. Cloke, *Pure Appl. Chem.*, 2001, **73**, 233–238.

63 W. T. Ford and J. B. Grutzner, ^1H and ^{13}C Nuclear Magnetic Resonance Spectra of Cyclopentadienylmagnesium Compounds in Tetrahydrofuran, *J. Org. Chem.*, 1972, **37**, 2561–2564.

64 P. Sobota and B. Duda, Influence of $MgCl_2$ on Grignard reagent composition in tetrahydrofuran. III, *J. Organomet. Chem.*, 1987, **332**, 239–245.

65 N. A. Jenek, A. Helbig, S. M. Boyt, S. B. Reeksting, G. Kociok-Köhn, H. Helten and U. Hintermair, The coming of age: Understanding and tuning the electronic structure of pentalenides, *ChemRxiv*, **2023**.

66 P. Zhao, C. D. Incarvito and J. F. Hartwig, Direct observation of β-aryl eliminations from Rh(I) alkoxides, *J. Am. Chem. Soc.*, 2006, **128**, 3124–3125.

67 S. Sakamoto, T. Taniguchi, Y. Sakata, S. Akine, T. Nishimura and K. Maeda, Chain: Catalysts for Living Polymerization of Phenylacetylene and Potential Helical Chirality of 1,3,5-Hexatrienes, *Helical Struct.*, 2021, **60**, 22201–22206.

68 T. Osswald, I. S. Mikhel, H. Rüegger, P. Butti and A. Mezzetti, Secondary ligand–metal interactions in rhodium(III) and iridium(III) phosphoramidite complexes, *Inorg. Chim. Acta*, 2010, **363**, 474–480.

69 J. W. Faller, R. H. Crabtree and A. Habib, Control of Slippage and Conformation in Indenyl Complexes, *Organometallics*, 1985, **4**, 929–935.

70 J. L. Atwood, W. E. Hunter, D. C. Hrncir, E. Samuel, H. Alt and M. D. Rausch, Molecular Structures of the Bis(η^5-indenyl)dimethyl Derivatives of Titanium, Zirconium, and Hafnium, *Inorg. Chem.*, 1975, **14**, 1757–1762.

71 H. Adams, N. A. Bailey, B. E. Mann, B. F. Taylor, C. White and P. Yavari, Activation energies for molecular tumbling and cyclopentadienyl rotation in $[M(\eta^5\text{-}C_5H_5)(\eta^4\text{-cod})](M = $ Rh or Ir; cod = cyclo-octa-1,5-diene) and the X-ray crystal structure of and bonding in $[Rh(\eta^5\text{-}C_5H_5)(\eta^4\text{-cod})]$, *J. Chem. Soc., Dalton Trans.*, 1987, **9**, 1947–1951.

72 M. Graf, H. C. Böttcher, P. Mayer and M. Scheer, Synthesis and Molecular Structures of $[Rh(\eta^5\text{-}C_5H_5)(coe)_2]$ (coe = cis-cyclooctene) and $[Rh(\eta^5\text{-}C_5H_5)(\eta^4\text{-cod})]$ (cod = cis,cis-η,^{4}–1,5-cyclooctadiene), *Z. Anorg. Allg. Chem.*, 2017, **643**, 1323–1325.

73 I. Y. Ilyin, I. V. Mirzaeva, T. S. Sukhikh, D. V. Bonegardt and T. V. Basova, Study Of The Correlation Between The Structure Of The [Ir(cod)Cp] Complex and its Thermal Properties, *J. Struct. Chem.*, 2021, **62**, 1863–1871.

74 H. Schumann and S. Stenz, Carbonyl(diphenylcyclopentadienyl) and carbonyl(tetraphenylcyclopentadienyl) rhodium(ı) complexes, *Z. Naturforsch., B: J. Chem. Sci.*, 2001, **56**, 1293–1296.

75 T. Piou, F. Romanov-Michailidis, M. Romanova-Michaelides, K. E. Jackson, N. Semakul, T. D. Taggart, B. S. Newell, C. D. Rithner, R. S. Paton and T. Rovis, Correlating reactivity and selectivity to cyclopentadienyl ligand properties in Rh(ııı)-catalyzed C-H activation reactions: An experimental and computational study, *J. Am. Chem. Soc.*, 2017, **139**, 1296–1310.

76 F. A. Cotton, in *Multiple Bonds Between Metal Atoms*, ed. F. A. Cotton, C. A. Murillo and R. A. Walton, Springer-Verlag, 3rd edn, 2006, pp. 35–68.

77 L. Pauling, Atomic Radii and Interatomic Distances in Metals, *J. Am. Chem. Soc.*, 1947, **69**, 542–553.

78 P. Pyykkö, Strong closed-shell interactions in inorganic chemistry, *Chem. Rev.*, 1997, **97**, 597–636.

79 S. Bajo, M. G. Alférez, M. M. Alcaide, J. López-Serrano and J. Campos, Metal-only Lewis Pairs of Rhodium with s, p and d-Block Metals, *Chem. – Eur. J.*, 2020, **26**, 16833–16845.

80 S. Bajo, M. M. Alcaide, J. López-Serrano and J. Campos, Dehydrogenative Double C−H Bond Activation in a Germylene-Rhodium Complex, *Chem. – Eur. J.*, 2021, **27**, 16422–16428.

81 M. G. Alférez, J. J. Moreno, C. Maya and J. Campos, Polarized Au(ı)/Rh(ı) bimetallic pairs cooperatively trigger ligand non-innocence and bond activation, *Dalton Trans.*, 2023, **52**, 3835–3845.

82 M. Navarro, J. J. Moreno, M. Pérez-Jiménez and J. Campos, Small molecule activation with bimetallic systems: a landscape of cooperative reactivity, *Chem. Commun.*, 2022, **58**, 11220–11235.

83 B. Klingert and H. Werner, Basische Metalle, XLII. Die Metall-Basizität der Komplexe $C_5Me_5Rh(PMe_3)_2$, C_5Me_5Rh $(C_2H_4PMe_3$ und $C_5Me_5Rh(C_2H_4)P_2Me_4$: Neue Pentamethyl-cyclopentadienylrhodium(ı)- und -rhodium(ııı)-Verbindungen, *Chem. Ber.*, 1983, **116**, 1450–1462.

84 A. K. Swarnakar, M. J. Ferguson, R. McDonald and E. Rivard, Transition metal-mediated donor–acceptor coordination of low-oxidation state Group 14 element halides, *Dalton Trans.*, 2016, **45**, 6071–6078.

85 R. Bissert, H. Braunschweig, R. D. Dewhurst and C. Schneider, Metal-Only Lewis Pairs Based on Zerovalent Osmium, *Organometallics*, 2016, **35**, 2567–2673.

86 D. Lionetti, V. W. Day and J. D. Blakemore, Synthesis and Electrochemical Properties of Half-Sandwich Rhodium and Iridium Methyl Complexes, *Organometallics*, 2017, **36**, 1897–1905.

87 H. Nakai, K. Jeong, T. Matsumoto and S. Ogo, Catalytic C-F bond hydrogenolysis of fluoroaromatics by $[(\eta^5\text{-}C_5Me_5)$ Rh$^I(2,2'$-bipyridine)], *Organometallics*, 2014, **33**, 4349–4352.

88 M. Aresta and E. Quaranta, Synthesis, characterization and reactivity of $[Rh(bpy)(C_2H_4)Cl]$. A study on the reaction with C_1 molecules (CH_2O, CO_2) and $NaBPh_4$, *J. Organomet. Chem.*, 1993, **463**, 215–221.

89 J. Lutz, F. Hollmann, T. V. Ho, A. Schnyder, R. H. Fish and A. Schmid, Bioorganometallic chemistry: biocatalytic oxidation reactions with biomimetic NAD^+/NADH co-factors and $[Cp*Rh(bpy)H]^+$ for selective organic synthesis, *J. Organomet. Chem.*, 2004, **689**, 4783–4790.

90 S. I. Johnson, H. B. Gray, J. D. Blakemore and W. A. Goddard, Role of Ligand Protonation in Dihydrogen Evolution from a Pentamethylcyclopentadienyl Rhodium Catalyst, *Inorg. Chem.*, 2017, **56**, 11375–11386.

91 V. Ganesan, D. Sivanesan and S. Yoon, Correlation between the Structure and Catalytic Activity of [Cp*Rh (Substituted Bipyridine)] Complexes for NADH Regeneration, *Inorg. Chem.*, 2017, **56**, 1366–1374.

92 C. L. Pitman, O. N. L. Finster and A. J. M. Miller, Cyclopentadiene-mediated hydride transfer from rhodium complexes, *Chem. Commun.*, 2016, **52**, 9105–9108.

93 M. A. Wright and J. A. Wright, PhotoCORMs: CO release moves into the visible, *Dalton Trans.*, 2016, **45**, 6801–6811.

94 T. E. Bitterwolf, Protonation and dimerization reactions of cyclopentadienylrhodiumcarbonylphosphine and phosphite derivatives, *Inorg. Chim. Acta*, 1986, **122**, 175–184.

95 D. M. Haddleton and R. N. Perutz, Solution and matrix photochemistry of (η-cyclopentadienyl)bis(ethane) rhodium, *J. Chem. Soc., Chem. Commun.*, 1985, 1372–1374.

96 A. Bara-Estaún, C. L. Lyall, J. P. Lowe, P. G. Pringle, P. C. J. Kamer, R. Franke and U. Hintermair, Understanding Rh-catalysed Hydroformylation with Phosphite Ligands through Catalyst Speciation Analysis by Operando FlowNMR Spectroscopy, *ChemCatChem*, 2023, **15**, e202201204.

97 D. Milstein, cis-Hydridoacylrhodium(ııı) Complexes Not Stabilized by Chelation. Reductive Elimination and Decarbonylation, *Organometallics*, 1982, **1**, 1549–1551.

98 D. G. DeWit, Reactivity of mononuclear rhodium(ıı) compounds, *Coord. Chem. Rev.*, 1996, **147**, 209–246.

99 P. Paul, B. Tyagi, A. K. Bilakhiya, M. M. Bhadbhade and E. Suresh, Stable mononuclear rhodium(ıı) polypyridyl

complexes:synthesis, spectroscopic and structural characterisation, *J. Chem. Soc., Dalton Trans.*, 1999, 2009–2014.

100 M. P. García, M. V. Jiménez, A. Cuesta, C. Siurana, L. A. Oro, F. J. Lahoz, J. A. López, M. P. Catalán, A. Tiripicchio and M. Lanfranchi, Synthesis and reactivity of mononuclear (pentachlorophenyl)rhodium(II) complexes. Structural relevance of rhodium-o-chlorine secondary bonding, *Organometallics*, 1997, **16**, 1026–1036.

101 R. T. Hamazawa, T. Nishioka, I. Kinoshita, T. Takui, R. Santo and A. Ichimura, Thiacalix[3]pyridine produces a stable mononuclear rhodium(II) complex with mutual Jahn–Teller effect, *Dalton Trans.*, 2006, **60**, 1374–1376.

102 M. Feller, E. Ben-Ari, T. Gupta, L. J. W. Shimon, G. Leitus, Y. Diskin-Posner, L. Weiner and D. Milstein, Mononuclear Rh(II) PNP-type complexes. Structure and reactivity, *Inorg. Chem.*, 2007, **46**, 10479–10490.

103 D. A. Smith, D. E. Herbert, J. R. Walensky and O. V. Ozerov, Monomeric rhodium(II) complexes supported by a diarylamido/bis(phosphine) PNP pincer ligand and their reactivity toward dihydrogen, *Organometallics*, 2013, **32**, 2050–2058.

104 K. Fuchigami, N. P. Rath and L. M. Mirica, Mononuclear Rhodium(II) and Iridium(II) Complexes Supported by Tetradentate Pyridinophane Ligands, *Inorg. Chem.*, 2017, **56**, 9404–9408.

105 B. R. James and D. Mahajan, Bis(ditertiaryphosphine) complexes of rhodium(I). Synthesis, spectroscopy, and activity for catalytic hydrogenation, *Can. J. Chem.*, 1979, **57**, 180–187.

106 H. A. Bent, An appraisal of valence-bond structures and hybridization in compounds of the first-row elements, *Chem. Rev.*, 1961, **61**, 275–311.

107 D. P. Drolet and A. J. Lees, Solution Photochemistry of (η^5-C$_5$R$_5$)Rh(CO)$_2$ (R = H, Me) Complexes: Pathways for Potosubstitution and C-H/Si-H Bond Activation Reactions, *J. Am. Chem. Soc.*, 1992, **114**, 4186–4194.

108 G. M. Reisner, I. Bernal, M. D. Rausch, S. A. Gardner and A. Clearfield, On the cyclodimerization of acetylenes to cyclobutadiene problem: the synthesis, crystal and molecular structure of (η^5-cyclopentadienyl)-(η^4-1,2-diphenylcyclobuta[l]phenanthrene)rhodium, *J. Organomet. Chem.*, 1980, **184**, 237–254.

109 R. S. Dickson and H. P. Kirsch, The effects of bulky substituents in the reactions of alkynes with (η,-C$_5$H$_5$)M(CO)$_2$, M = Co or Rh, *Aust. J. Chem.*, 1981, **34**, 1401–1411.

110 P. A. Corrigan, R. S. Dickson, S. H. Johnson, G. N. Pain and M. Yeoh, The role of binuclear rhodium complexes as possible intermediates in the formation of cyclopentadienone-rhodium complexes. Reactions between (η,-C$_5$H$_5$), Rh$_2$(CO)(CF$_3$C$_2$CF$_3$) and symmetrically disubstituted alkynes, *Aust. J. Chem.*, 1982, **35**, 2203–2214.

111 M. Kajitani, T. Suetsugu, R. Wakabayashi, A. Igarashi, T. Akiyama and A. Sugimori, An "adduct" between CpRh(S$_2$C$_2$Z$_2$) and ZC≡CZ (Z = COOCH$_3$) as an intermediate in CpRh(I)-catalyzed synthesis of tetramethyl-2,3,4,5-thiophenetetracarboxylate from elemental sulfur and ZC≡CZ, *J. Organomet. Chem.*, 1985, **293**, C15–C18.

112 M. Kajitani, R. Ochiai, R. Kikuchi, M. Okubo, T. Akiyama and A. Sugimori, Formation of (η-cyclopentadienyl)(1,2-disubstituted 1,2-ethylenedithiolato)cobalt(III) and -rhodium (III) in reactions of (η-cyclopentadienyl)cobalt(I) or -rhodium(I) species with 1,4-dithiins, *Polyhedron*, 1990, **9**, 1123–1125.

113 M. Nomura, H. Hatano, T. Fujita, Y. Eguchi, R. Abe, M. Yokoyama, C. Takayama, T. Akiyama, A. Sugimori and M. Kajitani, Formation, structure, and reactivities of 1 : 1 adducts between quadricyclane and (η^5-cyclopentadienyl)(1,2-diphenyl- or -dimethoxycarbonyl-1,2-ethenedithiolato)rhodium(III), *J. Organomet. Chem.*, 2004, **689**, 997–1005.

114 D. A. Lesch and T. B. Rauchfuss, Synthesis, Reactivity, and ^{125}Te NMR Studies of (C$_5$H$_5$)RhFe$_2$Te$_2$(CO)$_x$ (x = 6, 7), *Inorg. Chem.*, 1983, **22**, 1854–1857.

115 J. Washington and J. Takats, Alternative Synthesis and Fluxional Behavior of triangulo-Os$_2$Rh(CO)$_9$(C$_5$R$_5$) (R = H, Me), *Organometallics*, 1990, **9**, 925–928.

116 J. Tönnemann, J. Risse, Z. Grote, R. Scopelliti and K. Severin, Efficient and Rapid Synthesis of Chlorido-Bridged Half-Sandwich Complexes of Ruthenium, Rhodium, and Iridium by Microwave Heating, *Eur. J. Inorg. Chem.*, 2013, **2013**, 4558–4562.

117 J. L. Herde, J. C. Lambert, C. V. Senoff and M. A. Cushing, Cyclooctene and 1,5-Cyclooctadiene Complexes of Iridium (I), *Inorg. Synth.*, 2007, **15**, 18–20.

118 P. A. Boeg, J. Ø. Duus, J. H. Ardenkjær-Larsen, M. Karlsson and S. Mossin, Real-Time Detection of Intermediates in Rhodium-Catalyzed Hydrogenation of Alkynes and Alkenes by Dissolution DNP, *J. Phys. Chem. C*, 2019, **123**, 9949–9956.